

LOCKHEED MARTIN ENERGY RESEARCH LIBRARIES



3 4456 0509596 4

CENTRAL RESEARCH LIBRARY  
ORNL/TM-5328

Cy 83

## Selected Studies in HTGR Reprocessing Development

K. J. Notz

OAK RIDGE NATIONAL LABORATORY  
CENTRAL RESEARCH LIBRARY  
DOCUMENT COLLECTION  
**LIBRARY LOAN COPY**

DO NOT TRANSFER TO ANOTHER PERSON

If you wish someone else to see this  
document, send in name with document  
and the library will arrange a loan.

UCN-7969  
(3 3-67)

# OAK RIDGE NATIONAL LABORATORY

OPERATED BY UNION CARBIDE CORPORATION FOR THE ENERGY RESEARCH AND DEVELOPMENT ADMINISTRATION

Printed in the United States of America. Available from  
National Technical Information Service  
U.S. Department of Commerce  
5285 Port Royal Road, Springfield, Virginia 22161  
Price: Printed Copy \$5.00; Microfiche \$2.25

This report was prepared as an account of work sponsored by the United States Government. Neither the United States nor the Energy Research and Development Administration, nor any of their employees, nor any of their contractors, subcontractors, or their employees, makes any warranty, express or implied, or assumes any legal liability or responsibility for the accuracy, completeness or usefulness of any information, apparatus, product or process disclosed, or represents that its use would not infringe privately owned rights.

ORNL/TM-5328  
UC-77

Contract No. W-7405-eng-26

CHEMICAL TECHNOLOGY DIVISION

SELECTED STUDIES IN HTGR REPROCESSING DEVELOPMENT

K. J. Notz

MARCH 1976

**NOTICE** This document contains information of a preliminary nature and was prepared primarily for internal use at the Oak Ridge National Laboratory. It is subject to revision or correction and therefore does not represent a final report.

OAK RIDGE NATIONAL LABORATORY  
Oak Ridge, Tennessee 37830  
operated by  
UNION CARBIDE CORPORATION  
for the  
ENERGY RESEARCH AND DEVELOPMENT ADMINISTRATION



3 4456 0509596 4



## CONTENTS

	<u>Page</u>
Abstract. . . . .	1
INTRODUCTION . . . . .	1
I. SMALL-SCALE HOT CELL BURNING STUDIES. . . . .	3
Equipment and Facilities. . . . .	3
RTE-7 Carbide Fuels (TRISO/TRISO) . . . . .	10
H-Capsule Oxide Fuels (BISO/BISO) . . . . .	14
RTE-2-3 Carbide Fuels (TRISO/BISO). . . . .	22
Vapor Transport Studies . . . . .	27
II. OFF-GAS CLEANUP . . . . .	30
KALC Process (Krypton Absorption in Liquid CO <sub>2</sub> ) . . . . .	30
Iodox Process Tests and System Studies. . . . .	44
III. ALTERNATE BURNER CONCEPT . . . . .	46
Experimental Demonstration of Feasibility . . . . .	46
Evaluation and Theoretical Studies. . . . .	50
Gas Recycle Burner Studies. . . . .	51
IV. SOLVENT EXTRACTION. . . . .	56
Computer Modeling . . . . .	56
Experimental Tests; Sparging Effects. . . . .	58
V. WASTE PROCESSING AND ISOLATION. . . . .	62
Characterization Studies. . . . .	62
Fixation of <sup>14</sup> C as CaCO <sub>3</sub> . . . . .	67
Controlled Release of <sup>14</sup> CO <sub>2</sub> . . . . .	68
Acknowledgements. . . . .	69
References. . . . .	70



SELECTED STUDIES IN HTGR REPROCESSING DEVELOPMENT\*

K. J. Notz

## ABSTRACT

Recent work at ORNL on hot cell studies, off-gas cleanup, and waste handling is reviewed. The work includes small-scale burning tests with irradiated fuels to study fission product release, development of the KALC process for the removal of  $^{85}\text{Kr}$  from a  $\text{CO}_2$  stream, preliminary work on a non-fluidized bed burner, solvent extraction studies including computer modeling, characterization of reprocessing wastes, and initiation of a development program for the fixation of  $^{14}\text{C}$  as  $\text{CaCO}_3$ .

---

INTRODUCTION

Reprocessing of spent fuel is one step in the overall HTGR fuel cycle (Fig. 1); and in order to have a viable cycle, reprocessing must be successfully accomplished by a technology which is economically and environmentally acceptable. Thus, reprocessing development must follow closely behind reactor development. HTGR reprocessing development has been under way at the Oak Ridge National Laboratory, General Atomic Company, and KFA Jülich for up to 18 years and, more recently, at Allied Chemical Company. The major steps in HTGR reprocessing<sup>1</sup> are the head-end steps (block crushing, primary and secondary burning, particle separation and crushing, and dissolution); feed adjustment and solvent extraction; off-gas cleanup; and waste processing and isolation. Recent development work at ORNL has been in two major areas: (1) small-scale hot cell burning tests of irradiated fuel specimens, primarily to characterize fission product distributions in the off-gas; and (2) laboratory and engineering-scale development of the KALC process to remove  $^{85}\text{Kr}$  from the off-gas stream. More recently, work has been done on (3) an alternate burner concept, (4) solvent extraction, and (5) waste

---

\*Paper prepared for presentation at the AIChE Symposium on GCR Fuel Cycles, Atlantic City, Aug. 29 - Sept. 1, 1976.



processing and isolation. Selected topics from these five areas are presented in the following sections.

## I. SMALL-SCALE HOT CELL BURNING STUDIES

This work was performed with small specimens of various HTGR-type candidate fuels that had undergone irradiation equivalent to 20 to 50% burnup. Usually only small quantities of irradiated fuel were available, e.g., 1 to 4 fuel rods (1/2 in. x 2 in. each). This limited amount of material dictated limitations to the experimental procedures used and necessitated small-scale equipment, multiple sampling for diverse purposes, and rather complex experimental layouts. Also, it frequently precluded, or at least greatly restricted, the opportunity to perform duplicate experiments. With these limitations in mind, it is clear that the results cannot be completely definitive, but rather indicative of general behavior and trends. Early developmental studies<sup>2</sup> were made with low burnup Dragon fuels<sup>3</sup> while more recent studies, described below, were done with test specimens irradiated in Peach Bottom or EBR-II.

### Equipment and Facilities

The operating equipment for this work is housed in a hot cell (Fig. 2), with ancillary equipment in an overhead penthouse equipped with glove ports. Some of the support facilities, such as gas supplies, ratemeters, and controllers are also shown in Fig. 2. One of the equipment flowsheets (used for the second RTE-7 experiment) is shown in Fig. 3. The complete materials flow for this experiment, including primary and secondary burning, separation of fertile and fissile fractions, grinding, and dissolution, is shown in Fig. 4. The burner used for this work is shown in Figs. 5 and 6. The figures also show the "top hat" assembly which contains two sintered metal filters. Crushing (of TRISO-coated particles) was done in a modified high-speed blender (Fig. 7).

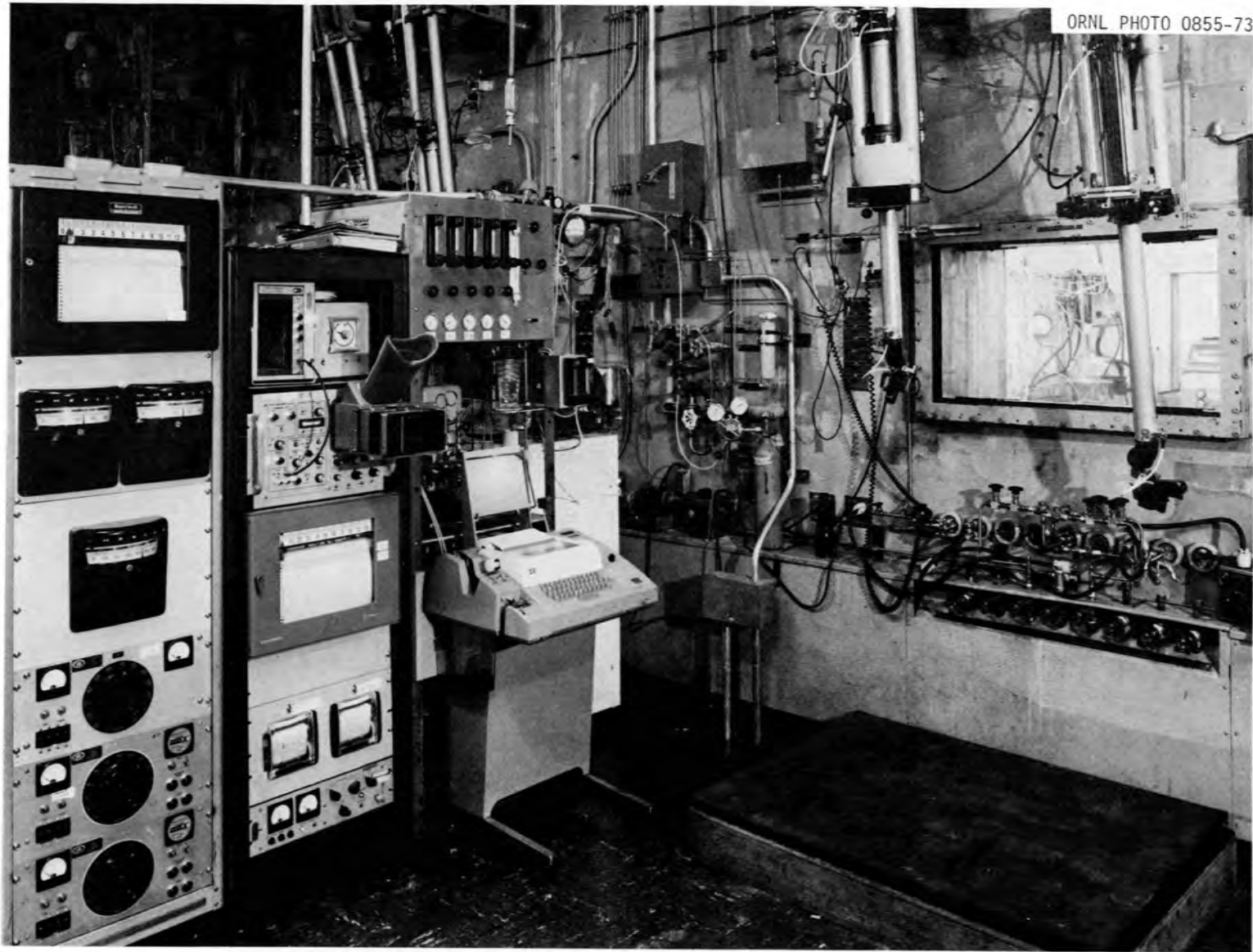


Fig. 2. Hot-Cell Facility for HTGR Small-Scale Burning Studies.

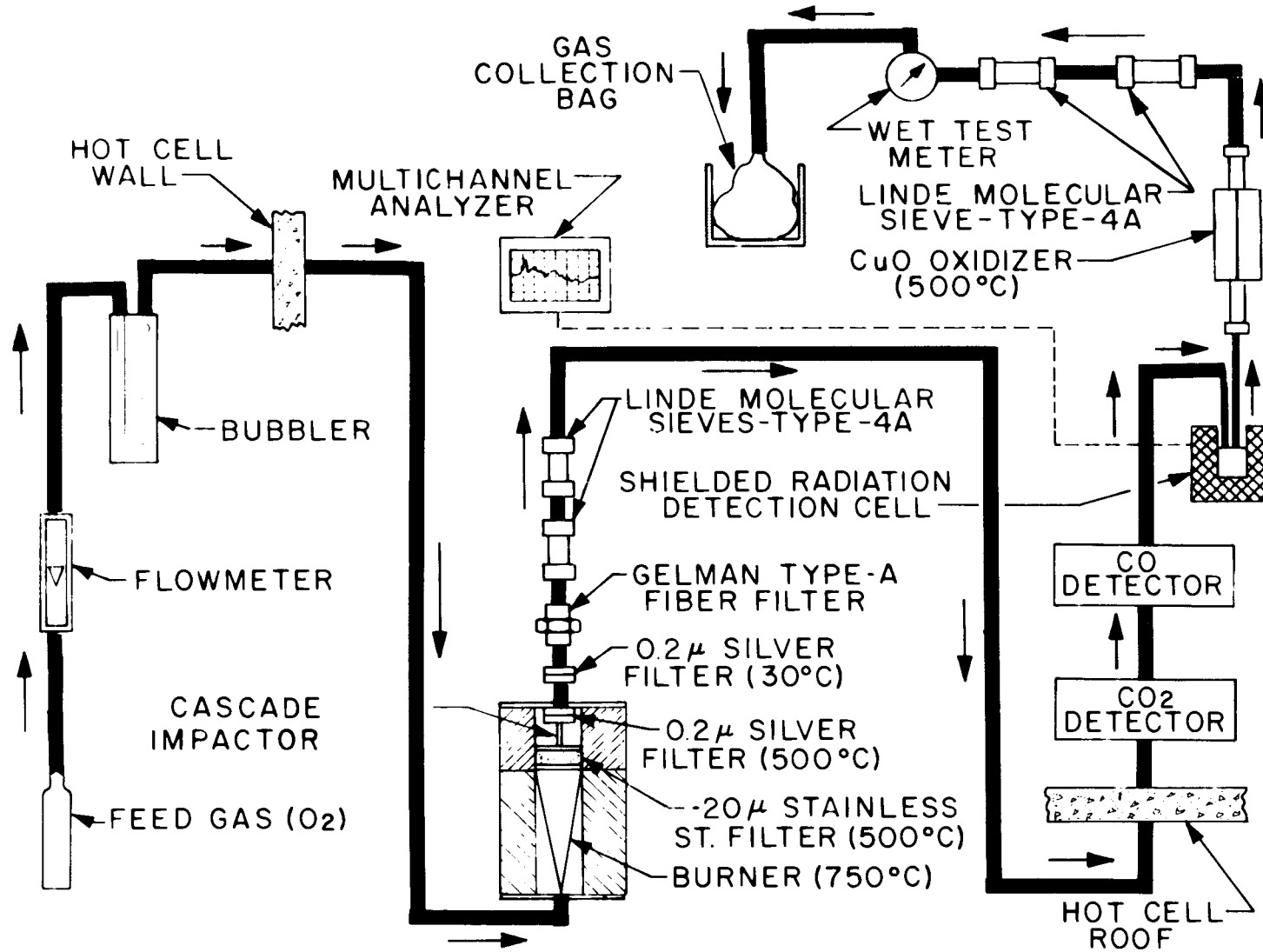


Fig. 3. Off-gas Train Used for RTE-7 Burning Studies with TRISO  $UC_2$ /TRISO  $ThC_2$  Fuel.

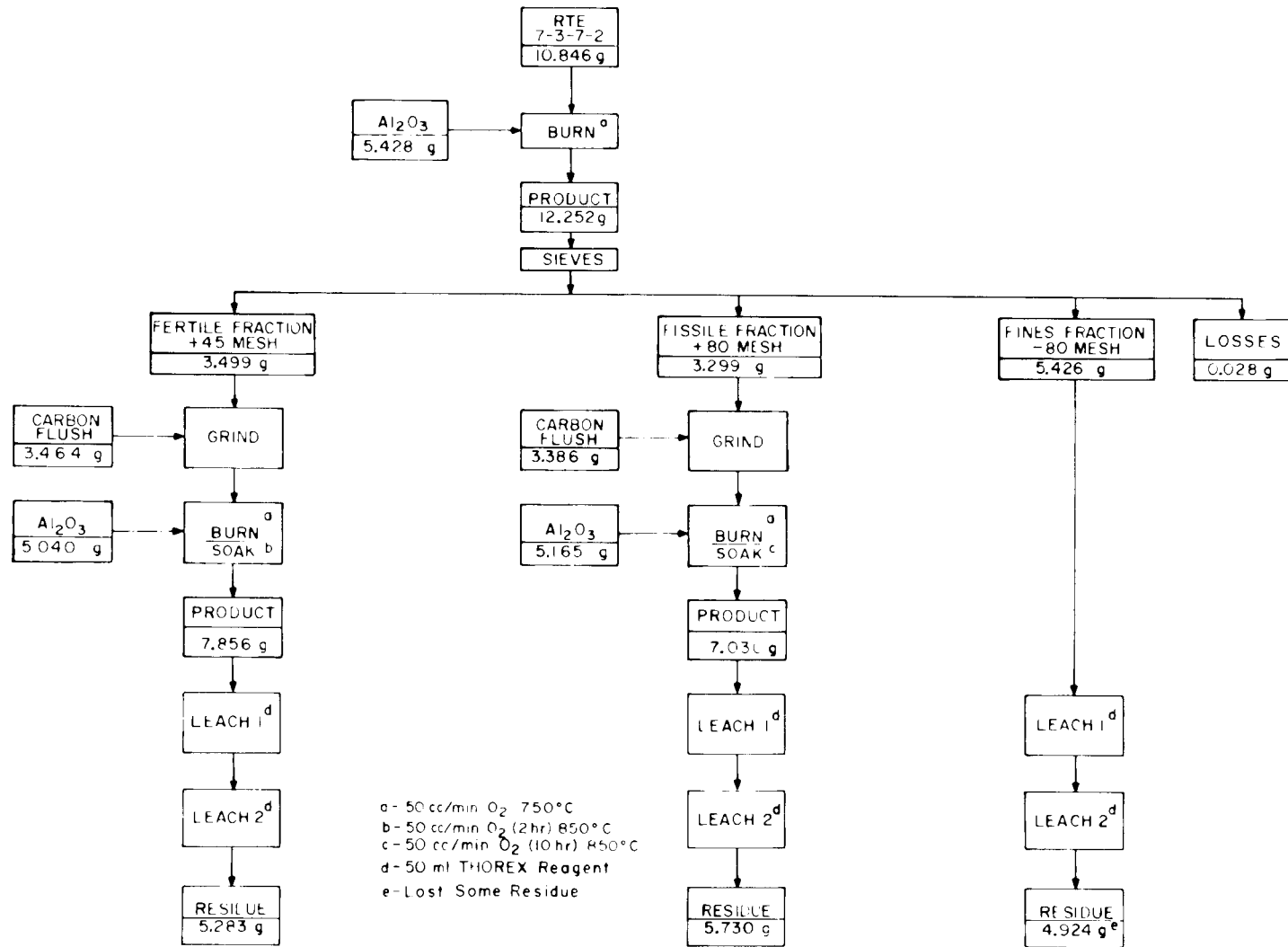


Fig. 4. Flowsheet Used for RTE-7 Studies with TRISO UC<sub>2</sub>/TRISO ThC<sub>2</sub> Fuel.

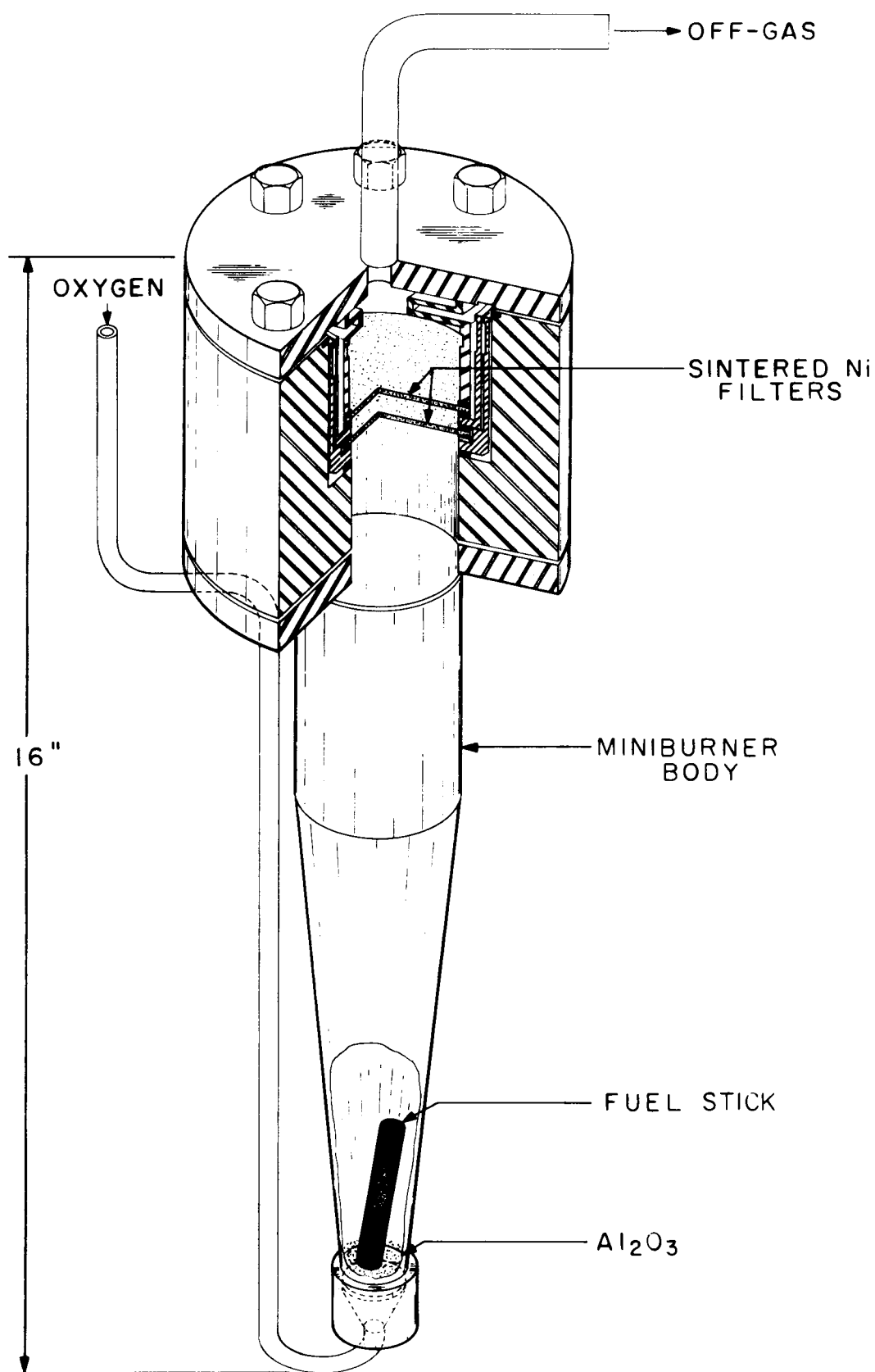


Fig. 5. Small-scale Burner and Filter Assembly.

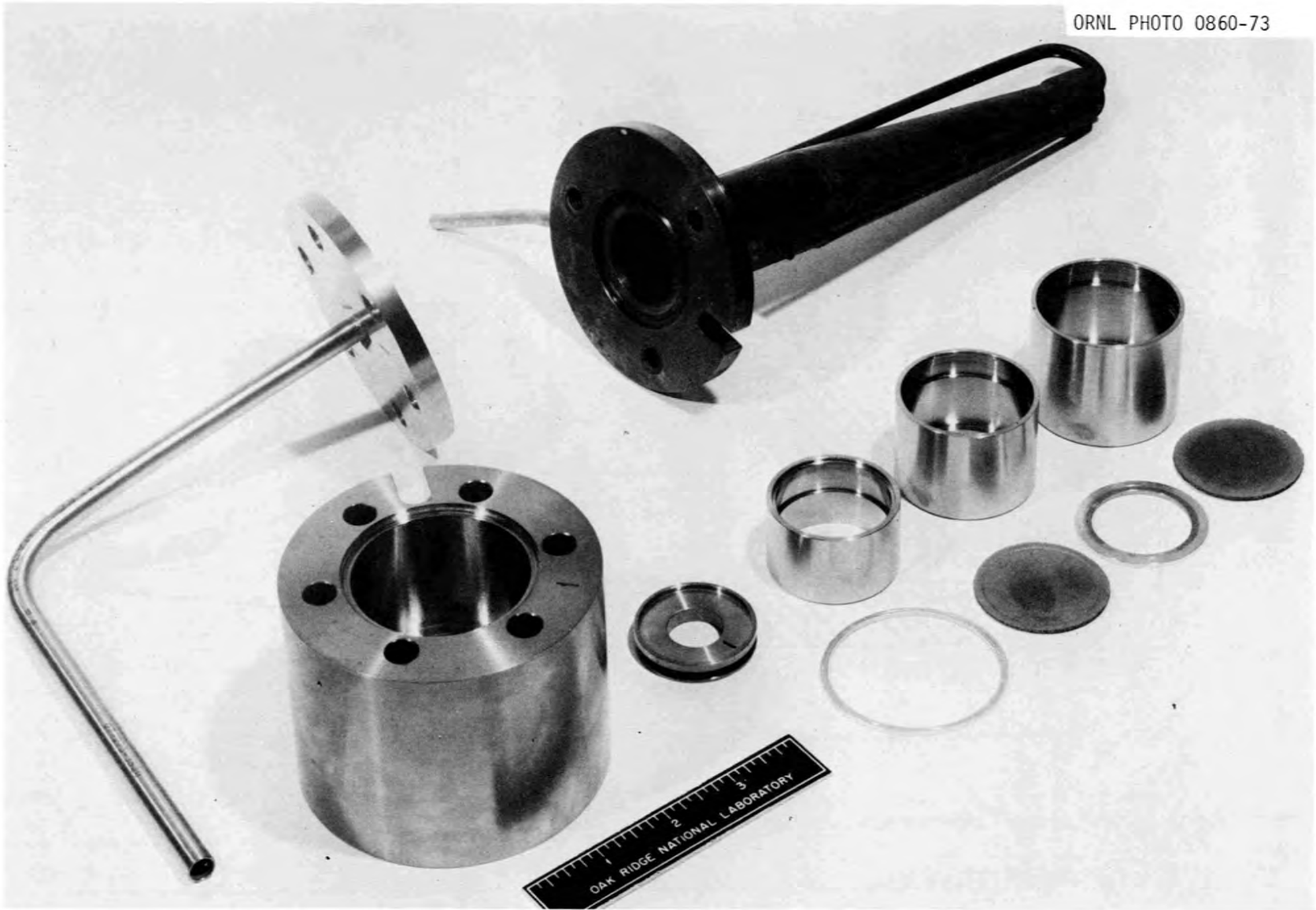


Fig. 6. Photo of Small-scale Burner and Filter Assembly.



Fig. 7. Controlled-Atmosphere Particle Crusher.

## RTE-7 Carbide Fuels (TRISO/TRISO)

Two complete experiments were performed with RTE-7 specimens,<sup>4</sup> which were TRISO UC<sub>2</sub>/TRISO ThC<sub>2</sub> type, contained in a rod matrix; only two rods were available. Results of the second experiment are presented here. In general, the first and second experiments agreed, but where they did not the second is considered to be the more reliable since it incorporated improvements in both equipment and technique designed to minimize uncontrolled hydrolysis, gas losses, etc. This fuel had a Th/U ratio of about 4, was exposed to a fast neutron fluence of about  $1.6 \times 10^{21} \text{ cm}^{-2}$  and a thermal neutron fluence of about  $1.2 \times 10^{21} \text{ cm}^{-2}$ . The burnup (FIMA) was calculated to be 20% for the fissile particles and 0.23% for the fertile particles.

The results in part are summarized in Tables 1-3. Table 1 shows the fractions of the various nuclides that were distributed between the off-gas train, dissolved in the leaches, and retained in the insoluble residues for all three burnings (primary, secondary-fissile, and secondary-fertile). Obviously, most of the activity was associated with the fissile particles. Of these nuclides, significant quantities of Ru (25%), Cs (6%), Sb (2%), and Nb-Zr (0.5 - 0.9%) were found in the off-gas train. Generally, the bulk of this activity in the off-gas train was retained on the sintered metal filters for the fissile fraction, with significant quantities being deposited downstream in the cold portion of the line (Table 2). For the primary and secondary-fertile burnings, almost all of the off-gas activity plated out on the cold line (Table 2). Returning to Table 1, for the primary burn more activity is found in the residues than in the leacher, while the reverse is true for both secondary burnings. Table 2 also shows <sup>75</sup>Se exclusively in the primary burning, trapped on the metal frit. This nuclide is an activation product, and the quantity found is equivalent to about 3 ppm natural Se in the fuel rod matrix.

Table 3 shows <sup>3</sup>H<sub>2</sub>O and <sup>85</sup>Kr releases. The krypton release is largely as expected: a small release during primary burning, indicating a small fraction of broken particles; a much larger release from the fissile than

Table 1. Fission product recoveries and main stream distribution for second RTE-7 experiment

	$^{95}_{\text{Zr}}$	$^{95}_{\text{Nb}}$	$^{106}_{\text{Ru}}$	$^{125}_{\text{Sb}}$	$^{134}_{\text{Cs}}$	$^{137}_{\text{Cs}}$	$^{144}_{\text{Ce}}$
Grand total, dpm	$1.532 \times 10^{10}$	$2.129 \times 10^{10}$	$1.266 \times 10^{11}$	$4.635 \times 10^{10}$	$1.983 \times 10^{11}$	$5.954 \times 10^{11}$	$3.800 \times 10^{12}$
Distribution (%)							
<u>Off-gas trains<sup>a</sup></u>							
Primary burn	0.03	< 0.01	0.01	< 0.01	< 0.01	0.01	0.01
Fertile burn	0.02	0.05	0.41	0.02	0.02	0.02	0.01
Fissile burn	0.89	0.42	25.23	2.08	6.01	6.06	0.02
Total	0.94	0.47	25.65	2.10	6.04	6.09	0.04
<u>Leaches</u>							
Primary burn fines <sup>b</sup>	0.06	0.07	0.02	0.04	0.04	0.04	0.03
Fertile particle ash <sup>c</sup>	4.58	6.73	4.96	4.77	1.81	3.58	2.28
Fissile particle ash <sup>c</sup>	75.92	70.91	26.64	69.21	73.29	71.82	87.03
Total	80.56	77.71	31.62	74.02	75.14	75.44	89.34
<u>Residues</u>							
Primary burn fines <sup>b</sup>	0.39	1.27	0.41	0.51	0.43	0.44	0.22
Fertile particle ash <sup>c</sup>	0.16	0.54	0.53	0.50	0.13	0.25	0.04
Fissile particle ash <sup>c</sup>	17.96	20.00	41.78	22.87	18.25	17.79	10.36
Total	18.51	21.81	42.72	23.88	18.81	18.48	10.62

<sup>a</sup>Includes sintered metal filter at top of burner.

<sup>b</sup>"Fines" includes broken particles and the Al<sub>2</sub>O<sub>3</sub> bed.

<sup>c</sup>"Ash" includes the Al<sub>2</sub>O<sub>3</sub> bed.

Table 2. Plateout and trapping of fission products in downstream off-gas equipment for second RTE-7 experiment

	<sup>95</sup> Nb	<sup>95</sup> Zr	<sup>106</sup> Ru	<sup>125</sup> Sb	<sup>134</sup> Cs	<sup>137</sup> Cs	<sup>144</sup> Ce	<sup>75</sup> Se
Total found in off-gas train (dpm)	1.004x10 <sup>8</sup>	1.446x10 <sup>8</sup>	3.250x10 <sup>10</sup>	9.708x10 <sup>8</sup>	1.197x10 <sup>10</sup>	3.627x10 <sup>10</sup>	1.589x10 <sup>9</sup>	9.738x10 <sup>5</sup>
Percent of grand total	0.47	0.94	25.65	2.10	6.04	6.09	0.042	100
Distribution within fractions								
<u>Initial burn<sup>a</sup> (μCi/liter)</u>	0.02	0.10	0.41	-	0.25	1.2	10.5(?)	0.02
SS frit No. 1, %	d	-	-	-	1.21	0.48	-	99.1
Hot Ag filter, %	-	-	-	-	-	-	-	0.9
Line leach, %	100	100	91.96	-	98.79	99.54	100	-
Cold Ag filter, %	No detectable gamma activity							
Gelman absolute filter, %	No detectable gamma activity							
<u>Fertile burn<sup>b</sup> (μCi/liter)</u>	0.16	0.04	7.8	0.13	0.47	1.4	2.4	-
SS frit No. 1, %	-	<3.74	5.10	-	0.90	1.48	7.76	-
SS frit No. 2, %	-	<0.75	1.28	-	0.06	0.06	1.17	-
Hot Ag filter, %	0.08	0.08	<0.01	-	0.01	0.01	0.12	-
Line leach, %	99.92	<95.43	93.61	100	99.03	98.45	90.91	-
Cold Ag filter, %	No detectable gamma activity							
Gelman absolute filter, %	No detectable gamma activity							
<u>Fissile burn<sup>c</sup> and soak (μCi/liter)</u>	0.85	1.3	306	9.2	114	345	8.8	-
SS frit No. 1, %	67.65	80.35	54.46	93.52	98.91	98.84	87.27	-
SS frit No. 2, %	26.86	17.24	35.68	4.88	0.99	1.05	7.57	-
Hot Ag filter, %	0.07	<0.22	0.53	0.03	<0.01	<0.01	<0.33	-
Line leach, %	5.43	2.19	9.33	1.56	0.11	0.12	4.83	-
Cold Ag filter, %	Trace of 0.24 MeV gamma activity							
Gelman absolute filter, %	Trace of 0.24 MeV gamma activity							

<sup>a</sup>Volume = 21.925 liters.

<sup>b</sup>Volume = 47.04 liters (with soak).

<sup>c</sup>Volume = 30.0 liters (with soak).

<sup>d</sup>Sought - not found (where dashes are shown).

Table 3. Fission gas release to the burner off-gas during processing of second RTE-7 experiment

	$^3\text{H}_2\text{O}$		$^{85}\text{Kr}$	
	dpm	%	dpm	%
Total	$1.746 \times 10^9$	100	$1.525 \times 10^{11}$	100
Initial burn		26.0		0.129
Fines leach		0.06		$\leq 0.010$
Fertile fraction (+45)				
Grind		0.06		0.221
Burn		13.23		3.220 <sup>a</sup>
Soak (2 hr)		0.21		b
Leach		0.02		$< 0.020$ <sup>b</sup>
Total		13.52		3.461
Fissile fraction (+80)				
Grind		0.01		19.016
Burn		56.47		77.377
Soak (2 hr)		2.24		b
Soak (8 hr)		1.66		b
Leach		0.04		0.125
Total		60.42		96.518

<sup>a</sup>Value is known to be low due to a leak in the CuO unit which occurred at the peak release time.

<sup>b</sup>Sought, not found.

from the fertile fraction; and significant release when the particles were crushed. The tritium release deviates from this pattern in several respects: 26% release during primary burning, indicating formation by activation (e.g., of Li) since  $^3\text{H}$  from ternary fission should be retained within the TRISO coatings; a relatively large fraction from the fertile particles (note, however, that the  $^{85}\text{Kr}$  result for the fertile particles may be low); and the delayed release of some of the tritium during prolonged thermal "soak" at temperature. Overall, including the thermal soak, 0.12% of the  $^3\text{H}$  was left in the leaches, for an overall DF of 830 from burning.

#### H-Capsule Oxide Fuels (BISO/BISO)

The H capsules contained BISO-coated oxide particles, irradiated to 8 to 31% FIMA with calculated maximum centerline temperatures of 1200 to 1430°C. Three fuel rods were burned (a single burn only, since all particles were BISO coated): one each with  $\text{UO}_2$ ,  $(2\text{Th,U})\text{O}_2$ , and  $(4\text{Th,U})\text{O}_2$  fissile kernels; all had  $\text{ThO}_2$  fertile particles. After burning, fertile and fissile fractions were separated on the basis of size. In this series,<sup>5</sup> the off-gas train (Fig. 8) was modified to include a five-stage cascade impactor (Fig. 9). The impactor was operated at 500°C and was preceded by a 20-micron sintered metal filter operated at a temperature > 500 but < 750°C. The characteristics of the impactor were such that it would deposit particles in the 1- to 7-micron range. The burning procedure was modified to provide information on  $^3\text{H}$  and  $^{85}\text{Kr}$  releases during the following sequence:

1. Hold at 850°C for 1 hr in Ar-4%  $\text{H}_2$  prior to burning.
2. Burn at a temperature of 750°C in moist air for the time required.
3. Hold at 850°C for 2 hr in moist air.
4. Hold at 850°C for 8 hr in moist air.
5. Reduction cycle in Ar-4%  $\text{H}_2$  for 6 hr at 850°C.
6. Oxidation cycle in moist  $\text{O}_2$  for 2 hr at 850°C.

The presence of  $\text{H}_2$  or water vapor at each stage was to provide isotopic dilution for  $^3\text{H}$ . A manifold with molecular sieve traps for  $^3\text{H}$  recovery

ORNL DWG. 75-15000RI

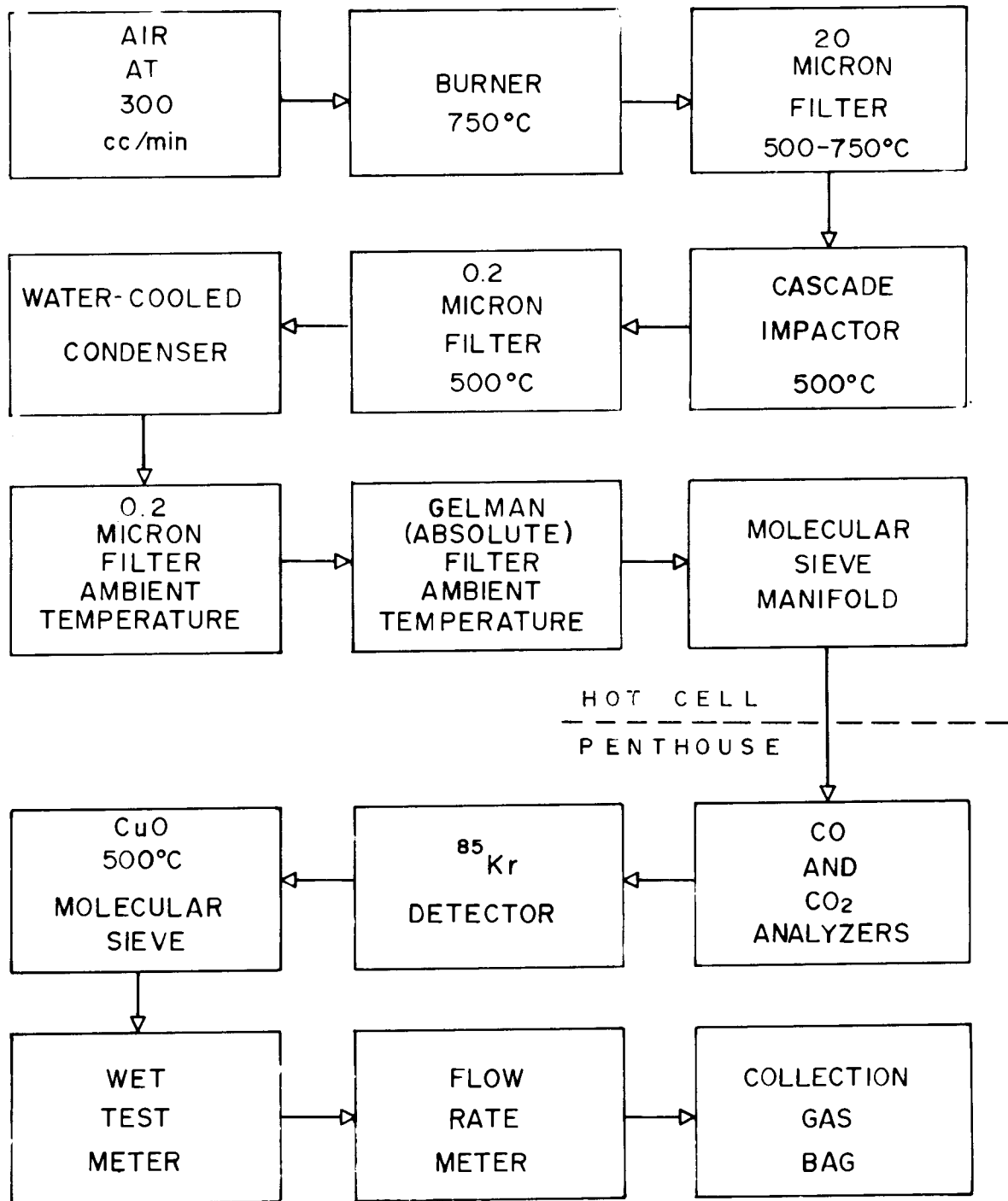


Fig. 8. Burning Flowsheet for H-Capsule Experiments with Oxide Fuels.

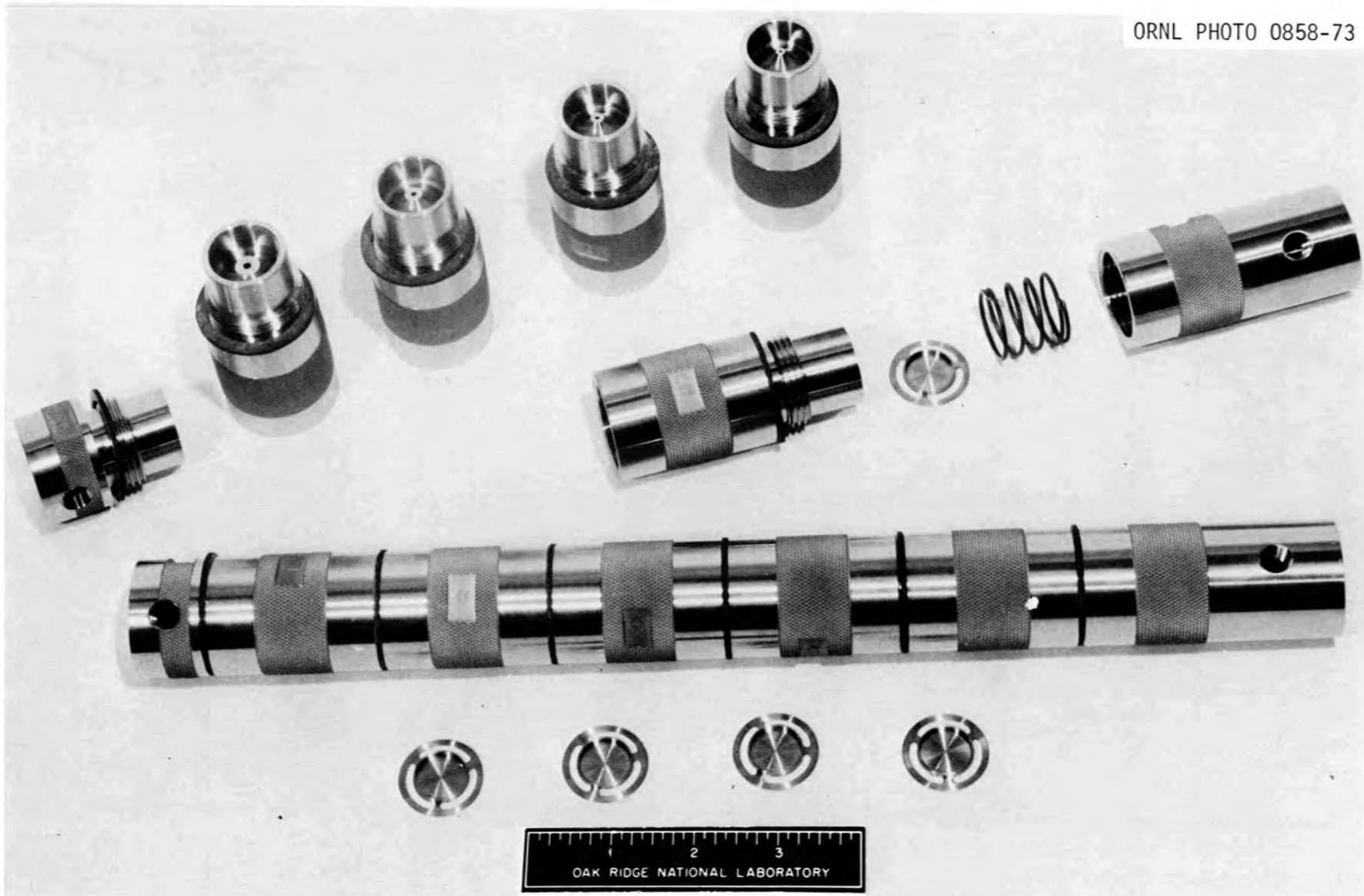


Fig. 9. Five-Stage Cascade Impactor.

was provided so that these could be changed after each stage. Additionally, the inflatable gas collection bag was changed at the end of each stage and samples taken for  $^{85}\text{Kr}$  analyses. The flow rates for each stage were 100 cc/min except the burning operation (step 2), which was done at 300 cc/min to provide the proper velocity for the cascade impactor. Dissolution procedures were also modified to test for selective dissolution by first treating with concentrated nitric acid and then with Thorex reagent (concentrated nitric acid plus fluoride catalyst). There was some difficulty in interpreting these data because the sample identities were not known with complete certainty; thus, it was not attempted to pin-point variations among the three different fissile particles. Rather, only general conclusions were drawn.

The quantities of  $^3\text{H}$  and  $^{85}\text{Kr}$  released during the overall burning sequence are shown in Table 4. Significant  $^3\text{H}$  release occurred during a long thermal soak, as well as during a subsequent reduction cycle for two of the samples. Krypton release also continued on into the soak period.

The off-gas profiles are similar to previous results. Most of the activity was on the first sintered metal filter; significant quantities plated out in the line where the temperature dropped from  $\approx 750^\circ\text{C}$  to  $500^\circ\text{C}$ . Relatively little activity was collected in the cascade impactor or in cold components downstream from the impactor. Yet, the final length of cold off-gas line contained appreciably activity. Results for one of the samples are given in Table 5. Within the impactor, activities generally decreased markedly after the first stage (Fig. 10).

The results of the dual leachings are shown in Table 6. All of the samples showed some selective solubility of the fissile uranium (vs bred U) in nitric acid, but only two gave a reasonably high solubility for fissile U [presumably the  $\text{UO}_2$  and  $(2\text{Th,U})\text{O}_2$  kernels]. However, in all cases excessive crossover occurs, and one concludes that concentrated nitric acid under these conditions is not selective enough to separate the  $^{233}\text{U}$  and  $^{235}\text{U}$  in this type of fuel.

Table 4. Fission gas releases for experiments with H-capsule oxide fuels

	$^{85}\text{Kr}$			$^3\text{H}$		
	H-2-2	H-2-3	H-2-4	H-2-2	H-2-3	H-2-4
Total for Exp. (dpm)	$1.36 \times 10^{11}$	$8.03 \times 10^{10}$	$1.62 \times 10^{11}$	$1.87 \times 10^9$	$2.57 \times 10^9$	$9.09 \times 10^8$
<u>% of total released in each operation:</u>						
Pre-burn soak (Ar-4% H <sub>2</sub> )	0.04	0.03	0.83	3.16	7.04	31.01
Burn (air)	77.71	49.22	59.82	67.92	64.49	47.28
2-hr soak (air)	1.92	8.57	1.52	5.34	25.94	3.10
8-hr soak (air)	0.37	0.79	0.86	11.66	1.68	7.53
Reduction cycle (Ar-4% H <sub>2</sub> )	0.15	0.19	0.33	8.18	0.40	8.86
Oxidation cycle (O <sub>2</sub> )	0.16	0.09	0.07	1.52	0.09	0.53
Fines (leaches)						
L-1 (HNO <sub>3</sub> )	0.20	Not done	0.03	1.36	Not done	0.15
L-2 (Thorex)	0.17	0.79	1.30	0.82	0.002	1.10
L-3 (Thorex)	0.07	-	0.06	-	-	0.26
Fertile (leaches)						
L-1 (HNO <sub>3</sub> )	3.29	0.21	0.04	0.01	0.12	0.06
L-2 (Thorex)	6.33	18.32	16.39	0.01	0.08	0.03
L-3 (Thorex)	0.82	0.22	0.07	-	0.03	< 0.01
Fissile (leaches)						
L-1 (HNO <sub>3</sub> )	0.15	11.16	0.10	0.01	0.03	< 0.01
L-2 (HNO <sub>3</sub> )	0.11	0.17	0.09	0.01	0.05	0.01
L-3 (Thorex)	7.05	9.61	18.42	< 0.01	0.04	0.06
L-4 (Thorex)	1.45	0.35	0.08	-	0.01	< 0.01

Table 5. Fission product concentration in burner off-gases for  
H-capsule experiment H-2-3

	$^{95}\text{Zr}$	$^{106}\text{Ru}$	$^{134}\text{Cs}$	$^{137}\text{Cs}$	$^{144}\text{Ce}$
Conc. in burner OG <sup>a</sup> ( $\mu\text{Ci/liter}$ )	0.93	122	98	441	10.7
% retained by:					
SS frit (< 750°C)	89.21	80.96	84.96	85.22	79.56
Hot OG line (500°C)	10.04	18.89	14.85	14.59	16.67
Impactor (500°C)	0.02	0.02	0.14	0.13	0.05
Hot Ag filter (500°C)	0.004	0.001	< 0.001	< 0.001	0.008
Condenser (20°C)	0.004	0.001	0.001	0.001	0.007
Cold Ag filter (RT)	0.004	0.001	< 0.001	< 0.001	0.008
Gelman filter (RT)	0.006	0.002	< 0.001	< 0.001	0.010
Cold OG line (RT)	0.68	0.12	0.06	0.06	.69

<sup>a</sup>Burning at 750°C in air at 300 cc/min. Burn includes a pre-burn hold at 850°C for 1 hr, and a post-burn hold at 850°C for 10 hr. Total volume for run was 133 liters.

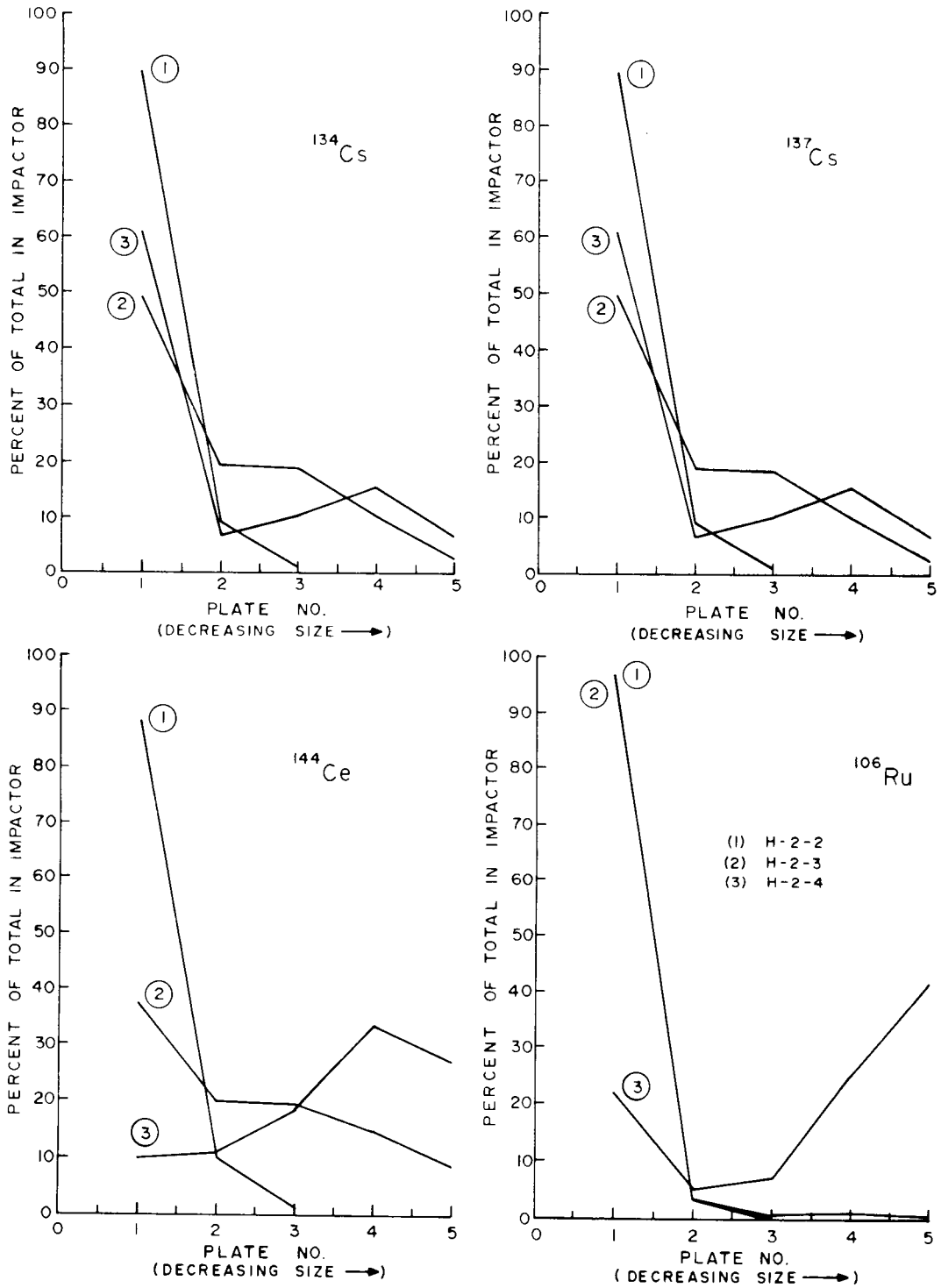


Fig. 10. Distribution of Fission Products Deposited in a Cascade Impactor for H-Capsule Experiments.

Table 6. Distribution of heavy metals in nitric acid and Thorex reagent leaches for H-capsule experiments

Nuclide	H-2-2		H-2-3		H-2-4	
	HNO <sub>3</sub> (%)	Thorex (%)	HNO <sub>3</sub> (%)	Thorex (%)	HNO <sub>3</sub> (%)	Thorex (%)
<sup>233</sup> U	39.61	60.41	17.66	82.34	7.13	92.87
<sup>234</sup> U	57.28	42.72	40.23	59.77	13.54	86.46
<sup>235</sup> U	86.06	13.94	95.83	4.17	28.56	71.44
<sup>236</sup> U	86.71	13.29	96.11	3.89	29.03	70.97
<sup>238</sup> U	85.92	14.08	96.01	3.99	32.38	67.62
Th	12.77	87.23	20.16	79.84	2.35	97.65

## RTE-2-3 Carbide Fuels (TRISO/BISO)

The RTE-2-3 fuel was irradiated to about 50% FIFAs as loose, blended beds of TRISO  $UC_2$ /BISO  $ThC_2$  to a maximum temperature of about 1340°C. Based on PIE, about 3 to 5% of the fissile particles had failed coatings, but the design limits of the SiC had been exceeded during the irradiation. In this test series,<sup>6,7</sup> the off-gas train (Fig. 11) was modified to test the effectiveness of 5-micron sintered metal filters at 500, 150, and 75°C after burning at 875°C. In these experiments, a relatively large amount of fine dust collected on the first filter (1 to 3 g from 63 g of coated particles) and was analyzed separately. In these runs it was not possible to separate fissile from fertile particles by sieving; therefore, the data represent mainly the primary burning of BISO fertile fuel, although the outer carbon was also burned from the TRISO particles, plus any contribution from the estimated 3 to 5% broken fertile particles.

All three experiments gave about the same results, showing about 10% of the total fission product activity in the dust on the filter, about 1 to 10% on the filter itself, and much less on the downstream components. Table 7 shows representative data from the run with the filter at 500°C; results at 150 and 75°C were quite similar. These results indicate that the bulk of the activity leaving the burning zone does so as particulate matter; also that any vapors of these fission products are largely condensed at 500°C. This dust is probably similar to the "fines" that must be recycled in a full-size burner. The concentration of activity in this dust is shown in Table 8 for all three runs. The filter decontamination factors are summarized in Table 9. The 150°C data appear to be slightly inconsistent with the 75° and 500° results, but in general:

1. Releases of measured fission products through a 5- $\mu$ m sintered nickel frit were of the order  $\leq 0.1\%$  to  $\leq 1.0\%$  of the inventory.
2. Experiments at three filter temperatures (500°C, 150°C, and 75°C) indicated less than one order of magnitude difference in release of fission products through the sintered nickel frit over these temperatures.

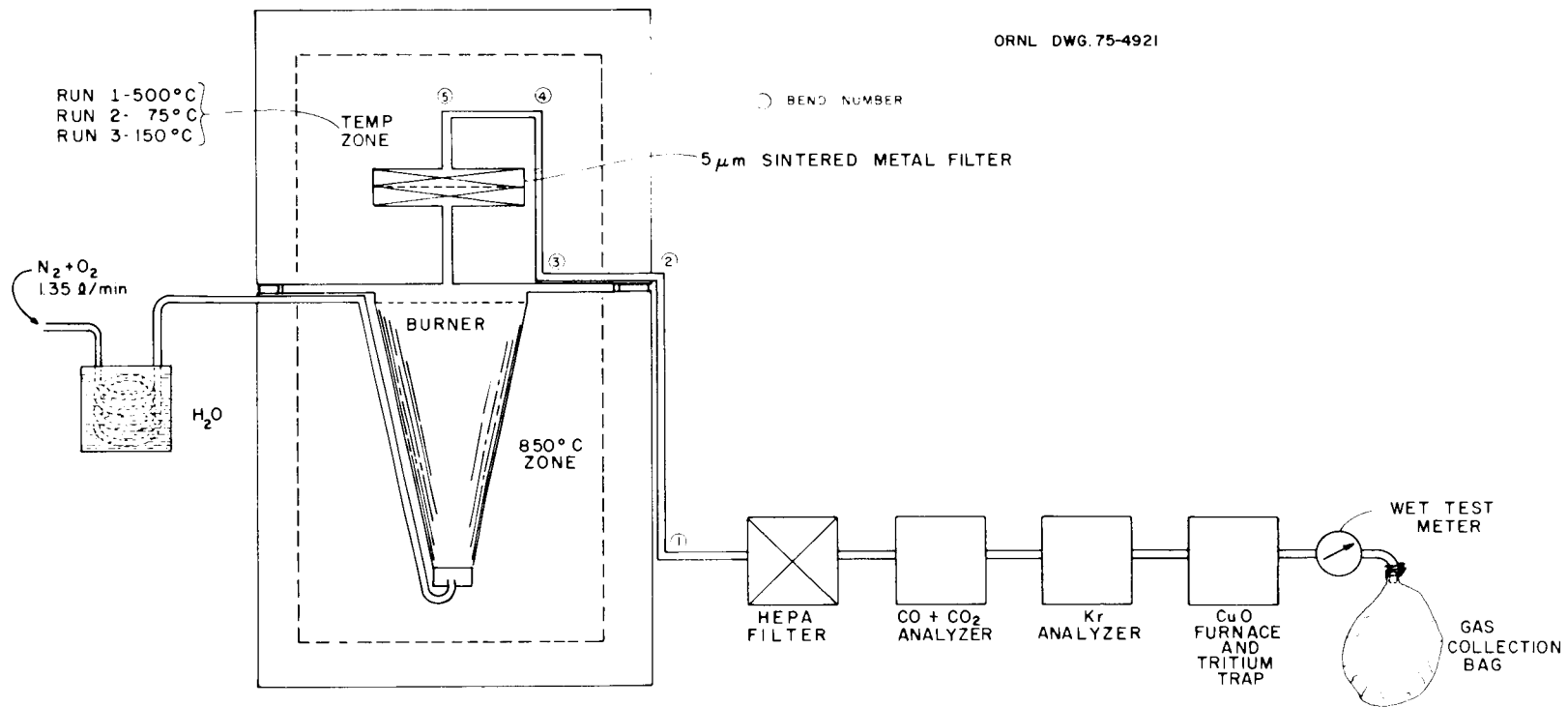


Fig. 11. Flowsheet for Burning with RTE 2-3 Carbide Fuel.

Table 7. Total amounts of gamma emitters found after burning 63 grams of coated particles from RTE-2-3 carbide fuel

Burner operated at 875°C with fluidizing gas (N<sub>2</sub> + O<sub>2</sub>) at 1 fps, 5-μm filter at 500°C

Gamma emitter	Burner <sup>a</sup> (dis/min)	Dust <sup>b</sup> (dis/min)	5-μm filter (dis/min)	OG lines (dis/min)	Abs. filter (dis/min)
<sup>95</sup> Zr	1.46 x 10 <sup>10</sup>	9.86 x 10 <sup>9</sup>	2.95 x 10 <sup>9</sup>	2.64 x 10 <sup>6</sup>	1.40 x 10 <sup>4</sup>
<sup>95</sup> Nb	7.11 x 10 <sup>11</sup>	1.84 x 10 <sup>10</sup>	5.74 x 10 <sup>9</sup>	7.78 x 10 <sup>6</sup>	2.97 x 10 <sup>4</sup>
<sup>106</sup> Ru	4.15 x 10 <sup>11</sup>	3.47 x 10 <sup>10</sup>	3.30 x 10 <sup>9</sup>	2.88 x 10 <sup>6</sup>	2.06 x 10 <sup>4</sup>
<sup>125</sup> Sb	1.27 x 10 <sup>11</sup>	5.91 x 10 <sup>9</sup>	8.70 x 10 <sup>8</sup>	9.27 x 10 <sup>5</sup>	5.18 x 10 <sup>4</sup>
<sup>134</sup> Cs	9.03 x 10 <sup>11</sup>	5.17 x 10 <sup>10</sup>	3.13 x 10 <sup>9</sup>	3.38 x 10 <sup>6</sup>	1.24 x 10 <sup>4</sup>
<sup>137</sup> Cs	1.50 x 10 <sup>12</sup>	8.94 x 10 <sup>10</sup>	5.28 x 10 <sup>9</sup>	6.27 x 10 <sup>6</sup>	2.07 x 10 <sup>4</sup>
<sup>144</sup> Ce	3.79 x 10 <sup>10</sup>	5.17 x 10 <sup>9</sup>	2.59 x 10 <sup>10</sup>	2.66 x 10 <sup>7</sup>	1.72 x 10 <sup>6</sup>

<sup>a</sup>Includes material from ThO<sub>2</sub> ash plus material on perforated plate inside burner. Material inside SiC-coated UC<sub>2</sub> particles is not included.

<sup>b</sup>Dust trapped on inlet side of 5-μm filter.

Table 8. Concentrations of fission products (in dis/min/g) from RTE-2-3 carbide fuel in the fine dust collected on a 5- $\mu$ m sintered metal filter held at various temperatures

Fission product	Run 1 (500°C filter)	Run 3 (150°C filter)	Run 2 (75°C filter)
$^{95}\text{Zr}$	$2.90 \times 10^9$	$\leq 1.49 \times 10^9$	$\leq 8.22 \times 10^8$
$^{95}\text{Nb}$	$5.41 \times 10^9$	$4.00 \times 10^{10}$	$3.44 \times 10^{10}$
$^{106}\text{Ru}$	$1.02 \times 10^{10}$	$6.45 \times 10^{10}$	$3.27 \times 10^{10}$
$^{125}\text{Sb}$	$1.74 \times 10^9$	$8.18 \times 10^9$	$6.05 \times 10^9$
$^{134}\text{Cs}$	$1.52 \times 10^{10}$	$3.83 \times 10^{10}$	$3.00 \times 10^{10}$
$^{137}\text{Cs}$	$2.63 \times 10^{10}$	$6.68 \times 10^{10}$	$5.13 \times 10^{10}$
$^{144}\text{Ce}$	$1.52 \times 10^9$	$\leq 1.94 \times 10^9$	$\leq 1.61 \times 10^8$

Table 9. Decontamination factors across a 5- $\mu\text{m}$  sintered-metal filter held at various temperatures for RTE-2-3 carbide fuel

Fission product	Temperature of 5- $\mu\text{m}$ filter ( $^{\circ}\text{C}$ )	Overall DF <sup>a</sup> across filter	Filter DF <sup>b</sup>
<sup>95</sup> Zr	500	7,500	3,500
	150	10,500	400
	75	32,000	4,700
<sup>95</sup> Nb	500	94,000	3,100
	150	55,300	4,100
	75	220,000	23,000
<sup>106</sup> Ru	500	150,000	13,100
	150	277,000	17,600
	75	960,000	40,000
<sup>125</sup> Sb	500	140,000	6,900
	150	6,500	440
	75	260,000	2,100
<sup>134</sup> Cs	500	280,000	16,000
	150	133,000	8,600
	75	570,000	52,000
<sup>137</sup> Cs	500	250,000	15,000
	150	135,000	9,600
	75	460,000	43,000
<sup>144</sup> Ce	500	2,400	1,100
	150	2,200	130
	75	25,000	6,800

<sup>a</sup>Overall DF =  $\frac{\text{grand total dis/min found}}{(\text{lines} + \text{absolute filter dis/min})}$  ; i.e., including the ash remaining in the burner.

<sup>b</sup>Filter DF =  $\frac{(\text{dust} + \text{frit} + \text{lines} + \text{absolute filter}) \text{ dis/min}}{(\text{lines} + \text{absolute filter}) \text{ dis/min}}$  ; i.e., excluding the ash.

3. The dust trapped by the sintered nickel frit contained most of the fission products (and/or burner ash fines) that left the burner. Recycle of this dust to the primary burner will return this material to the circuit.

Note that these runs do not provide information pertaining to long-term plate-out effects on the various surfaces.

The three RTE-2-3 burnings were also analyzed for  $^{14}\text{C}$  in the product gases (Table 10). Inspection of Table 10 shows that the  $^{14}\text{C}$  ratio was not constant, but peaked during the course of a burn, indicating non-uniform distribution of the  $^{14}\text{C}$  within the coated particles. Each burning sample contained about 3.4 g U and 16.3 g Th, or 19.7 g total heavy metals. On this basis, the  $^{14}\text{C}$  release is about 17 Ci/ton of HM. For comparison, the  $^{14}\text{C}$  content of fully irradiated HTGR fuel is calculated to be about 12 Ci/ton for fuel with about 26 ppm  $\text{N}_2$  (total fuel basis: HM plus graphite). About 100 ppm  $\text{N}_2$  overall would be required to yield the 17 Ci/ton observed here (for fuel at about 40% of full burnup) for the kernels only, which is roughly equivalent to 800 ppm  $\text{N}_2$  in the coated fuel particles (which were our only source of  $^{14}\text{C}$  in these runs). However, these results are not necessarily representative since later burnings with another RTE-2-3 sample yielded only 16  $\mu\text{Ci/g C}$ , while still another carbide fuel (RTE-2-6) yielded only 4  $\mu\text{Ci/g C}$ .

#### Vapor Transport Studies

An experimental program has been initiated to examine by tracer techniques the vapor transport of fission products and actinides from the burner off-gas during head-end burning.<sup>8</sup> This study will obtain data under controlled conditions on beta and alpha emitters (as well as gamma emitters) not easily analyzed for in hot cell studies. A transpiration method will be employed (Fig. 12), and various burner atmospheres (neutral, oxidizing, and reducing) will be applied. An isotope dilution method with mass assay will be used, which gives excellent sensitivity and accuracy. This method has the added advantages of avoiding radioactivity and being immune to physical losses once the mass tracer spike has been added and equilibrated.

Table 10. Concentrations of fission products (in dis/min/g) from RTE-2-3 carbide fuel in the fine dust collected on a 5- $\mu$ m sintered-metal filter held at various temperatures

Sample <sup>a</sup>	Run 1 (500°C)		Run 2 (75°C)		Run 3 (150°C)	
	C <sup>b</sup> (g)	<sup>14</sup> C ( $\mu$ Ci/g C)	C (g)	<sup>14</sup> C ( $\mu$ Ci/g C)	C (g)	<sup>14</sup> C ( $\mu$ Ci/g C)
1	0.67	10.2	1.44	3.8	1.03	7.2
2	1.72	27.3	2.58	42.6	2.00	43.1
3	1.87	36.0	3.11 <sup>c</sup>	51.4 <sup>c</sup>	2.25	73.0
4	1.66	46.8	2.69	14.6	2.18	-
5	3.32	21.6	2.53	7.4	2.29	7.5
6	2.36	11.4	0.45	11.0	2.04	5.8
Totals	11.59	25.7 <sup>d</sup>	12.81	26.4 <sup>d</sup>	12.15 <sup>e</sup>	~31 <sup>f</sup>

<sup>a</sup>Samples taken nominally ~ 30 min apart at nominal volumes of ~ 50 liters of off-gas.

<sup>b</sup>Carbon calculated from gas laws and CO<sub>2</sub> analyses.

<sup>c</sup>CO<sub>2</sub> concentration taken as the average of samples 2 and 4.

<sup>d</sup>Total <sup>14</sup>C found/total C found.

<sup>e</sup>A seventh sample had 0.36 g C but was not analyzed for <sup>14</sup>C.

<sup>f</sup>Sample 4 was omitted; also sample 7.

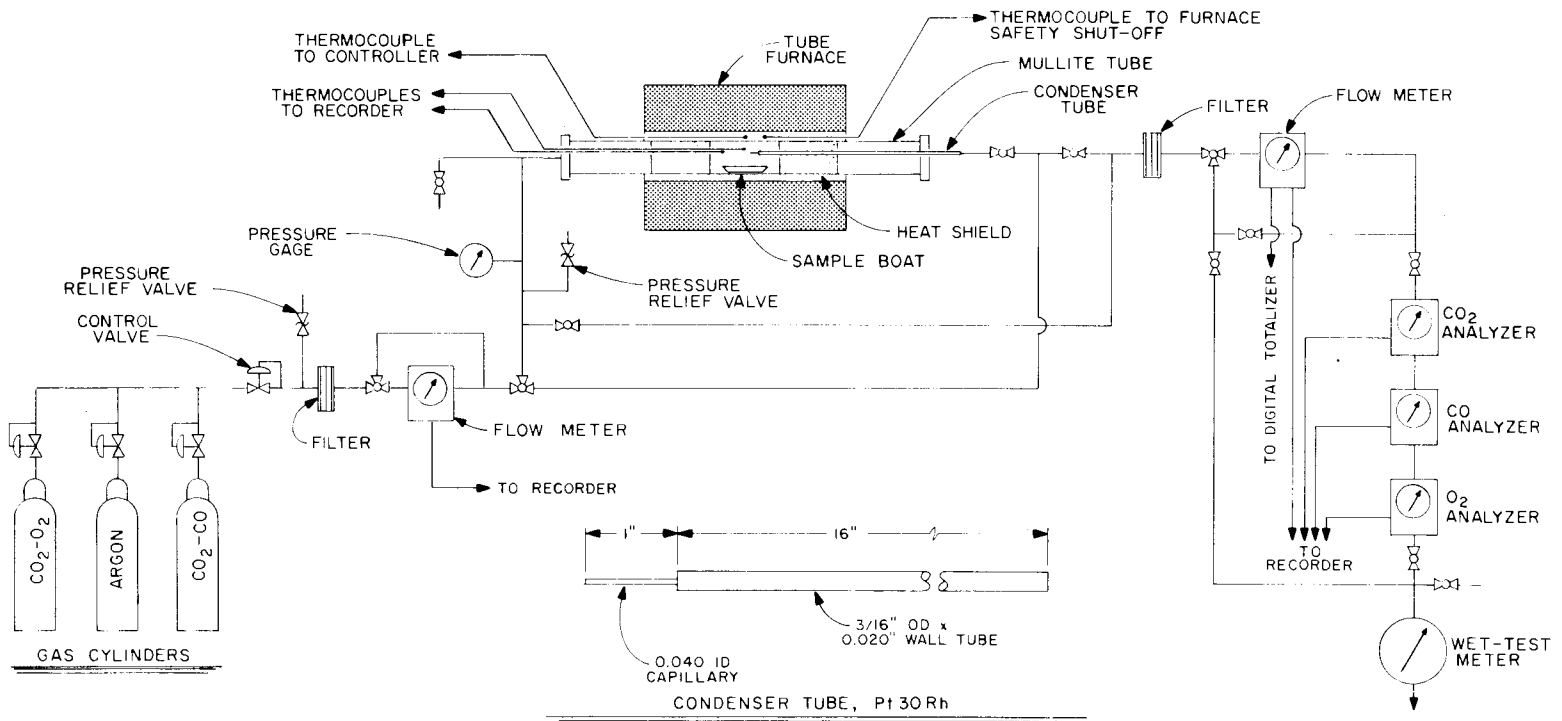


Fig. 12. Schematic Diagram of Transpiration Apparatus.

## II. OFF-GAS CLEANUP

The major source of off-gas is the primary burner, but other sources also contribute (e.g., the crushers, particle separators, dissolver, and instrument purges). The large CO<sub>2</sub> content (up to 90%) and the large volume (about 2000 SCFM for a commercial-size plant) distinguish HTGR fuel reprocessing off-gas from that for other fuel types. The CO<sub>2</sub> interferes with the processes normally used to concentrate <sup>85</sup>Kr out of an air stream, and a new process had to be developed. Off-gas cleanup also includes <sup>129,131</sup>I and <sup>3</sup>H removal, and holdup of <sup>220</sup>Rn long enough to permit essentially complete decay to solid products (about ten minutes is long enough for the holdup, since the half-life of <sup>220</sup>Rn is only 55 sec). A general flowsheet for off-gas cleanup is shown in Fig. 13, while Fig. 14 gives more detail. The quantities shown in Fig. 14 are for a pilot plant sized to handle the off-gas from 24 fuel elements per day. Iodine will be removed by silver zeolite (and perhaps lead zeolite also), radon will be held up on Zeolon 900 molecular sieve, tritiated water will be taken out with Linde molecular sieve type 3A, and krypton will be removed via the KALC (Krypton Absorption in Liquid CO<sub>2</sub>) process. The KALC process was developed at ORNL and will be described below. (A related process, AKUT, is being developed at KFA Jülich.<sup>9</sup>) The other processes are being developed at ACC. It was recently recognized that the small amounts of SO<sub>2</sub> released during fuel combustion might interfere with some of the planned off-gas treatment, and studies of this are underway at both ACC and ORNL. Tests on I<sub>2</sub> removal by the Iodox process and fundamental studies on the CO<sub>2</sub>-I<sub>2</sub>-H<sub>2</sub>O system were also conducted as part of this program.

### KALC Process (Krypton Absorption in Liquid CO<sub>2</sub>)

Several processes for removing ppm quantities of <sup>85</sup>Kr and other noble gases from various gas streams are available in current technology. However, these processes are not applicable to a large off-gas stream which is primarily CO<sub>2</sub> because of the many similarities between Kr and CO<sub>2</sub> in those physical properties (such as adsorption and solubility) that provide the

ORNL DWG 74-8019

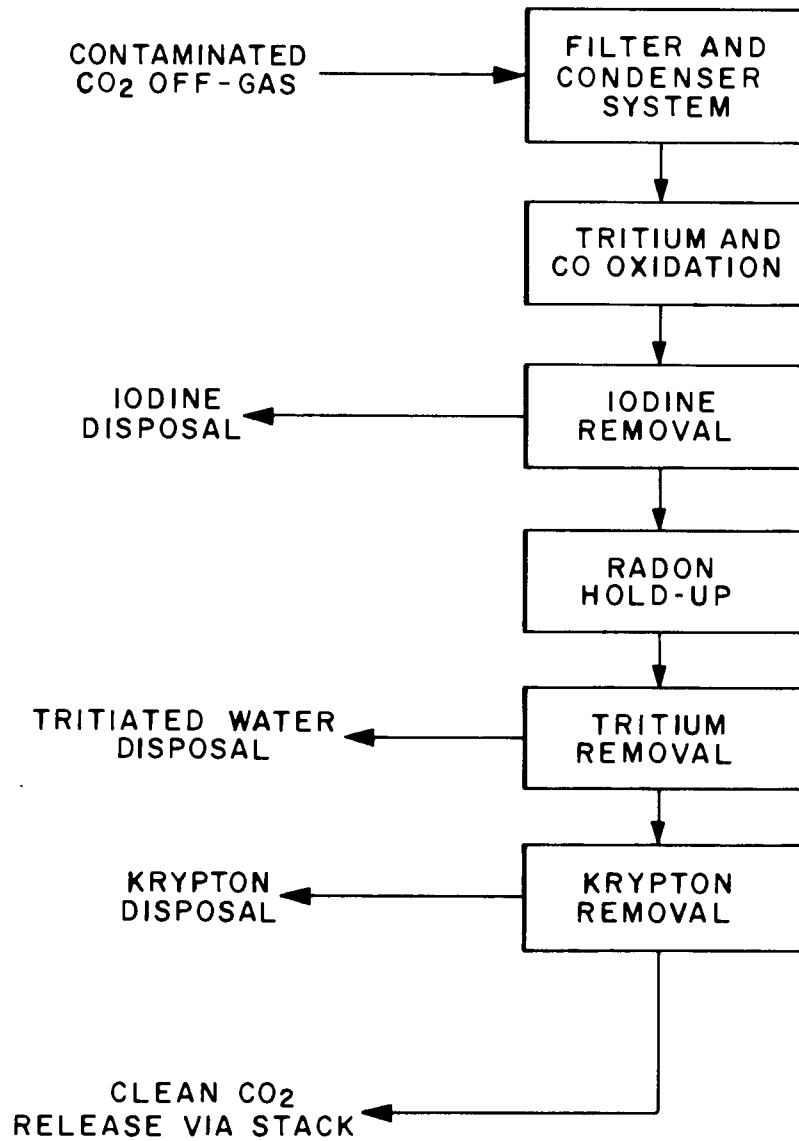


Fig. 13. General Flowsheet for Off-Gas Cleanup.

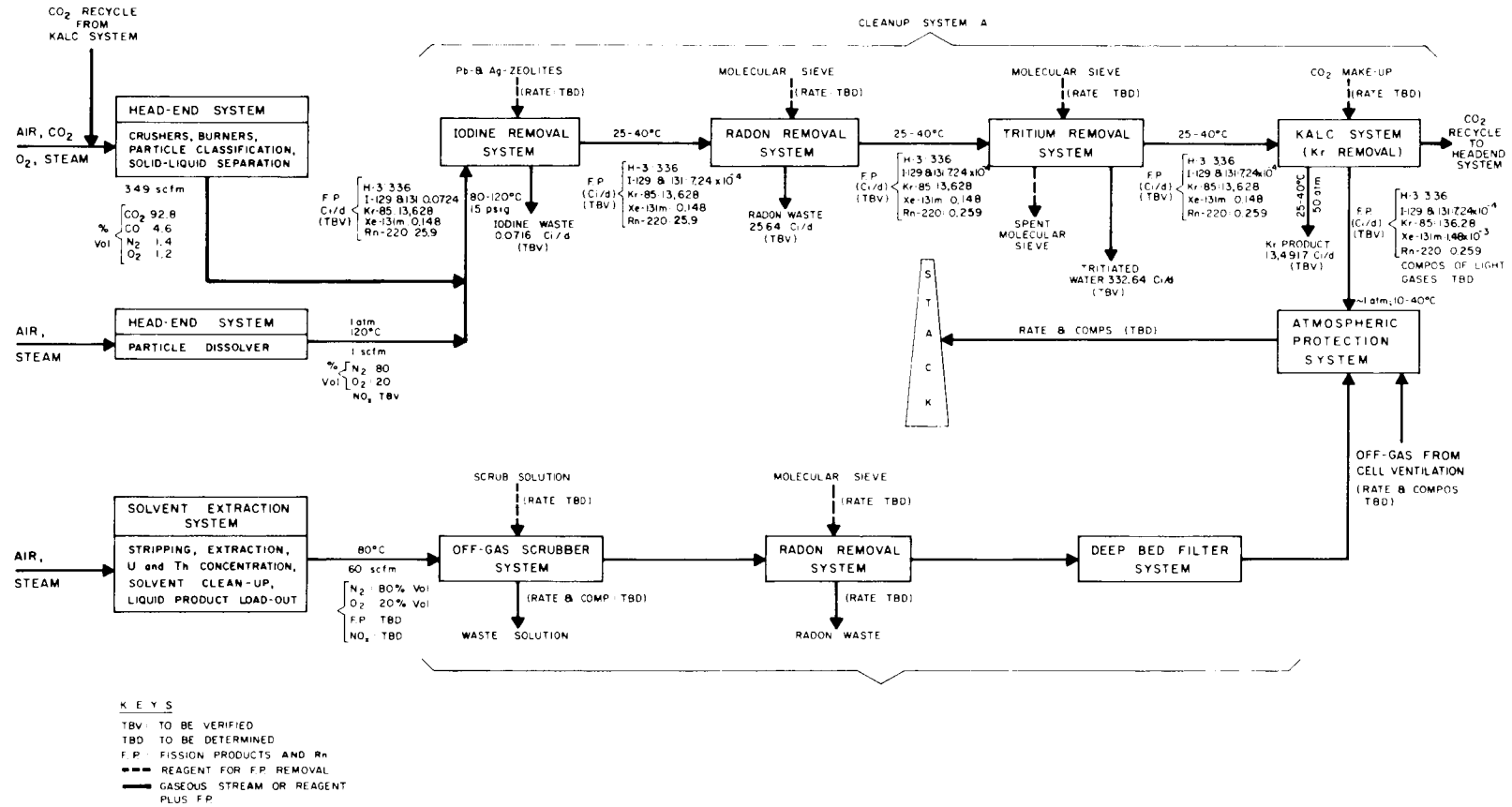


Fig. 14. Off-Gas System for Proposed HTGR Fuel Reprocessing Pilot Plant (Basis: 24 Fuel Blocks per Day).

basis for previously developed separation schemes.<sup>10</sup> By capitalizing on these similarities, the relatively high solubility of Kr in CO<sub>2</sub><sup>11</sup> provides the basis for separating Kr from the light gases (O<sub>2</sub>, N<sub>2</sub>, CO) present in the HTGR CO<sub>2</sub> off-gas, while a subsequent fractionation step separates the Kr from the liquid CO<sub>2</sub> solvent in the KALC process.<sup>12</sup> This process has the added advantage that the absorbent is one of the species already present in the gas mixture, thus avoiding the introduction of a new component. Furthermore, the KALC process may also provide a means to obtain additional decontamination for tritiated water, I<sub>2</sub>, and particulate matter during the scrubbing and fractionation steps.

The KALC process (Fig. 15) operates as follows: (1) incoming CO<sub>2</sub>, Kr, and light gases are chilled and scrubbed free of Kr with liquid CO<sub>2</sub>, while most of the light gases (along with some CO<sub>2</sub>) are discharged; (2) the liquid CO<sub>2</sub>, which now contains all the Kr and the balance of the light gases, is fractionated to remove these remaining light gases, which are then recycled to the scrubber because they contain some Kr; (3) the Kr-rich CO<sub>2</sub> is further fractionated to boil off the Kr, which is bottled and sent to storage for ultimate disposal; (4) the remaining liquid CO<sub>2</sub>, now free of both light gases and Kr, provides the scrubber liquid for the first step, plus an excess (corresponding to steady-state input of HTGR off-gas to the system) which is discharged. Xenon, which is also present in the burner off-gas in ppm amounts, will be carried with the Kr up to the final stripping step. Radioactive xenon, which is short-lived, will be largely decayed out prior to reprocessing, and only cold xenon will be present in significant quantities. Pilot studies have demonstrated the feasibility of the KALC operations. An early theoretical analysis<sup>13</sup> of the various steps shows that it should be practical to release no more than about 1% of the krypton and 30% of the xenon from the system with the decontaminated gaseous carbon dioxide waste; another 0.01% of the krypton and 67% of the xenon leave with a decontaminated liquid carbon dioxide waste. The remaining ~ 99% of the krypton will probably be compressed into a container, along with some CO<sub>2</sub> and xenon, and stored; to decrease the quantity of CO<sub>2</sub> in the Kr, a separate concentration step will be used. The decontaminated gaseous waste stream contains about

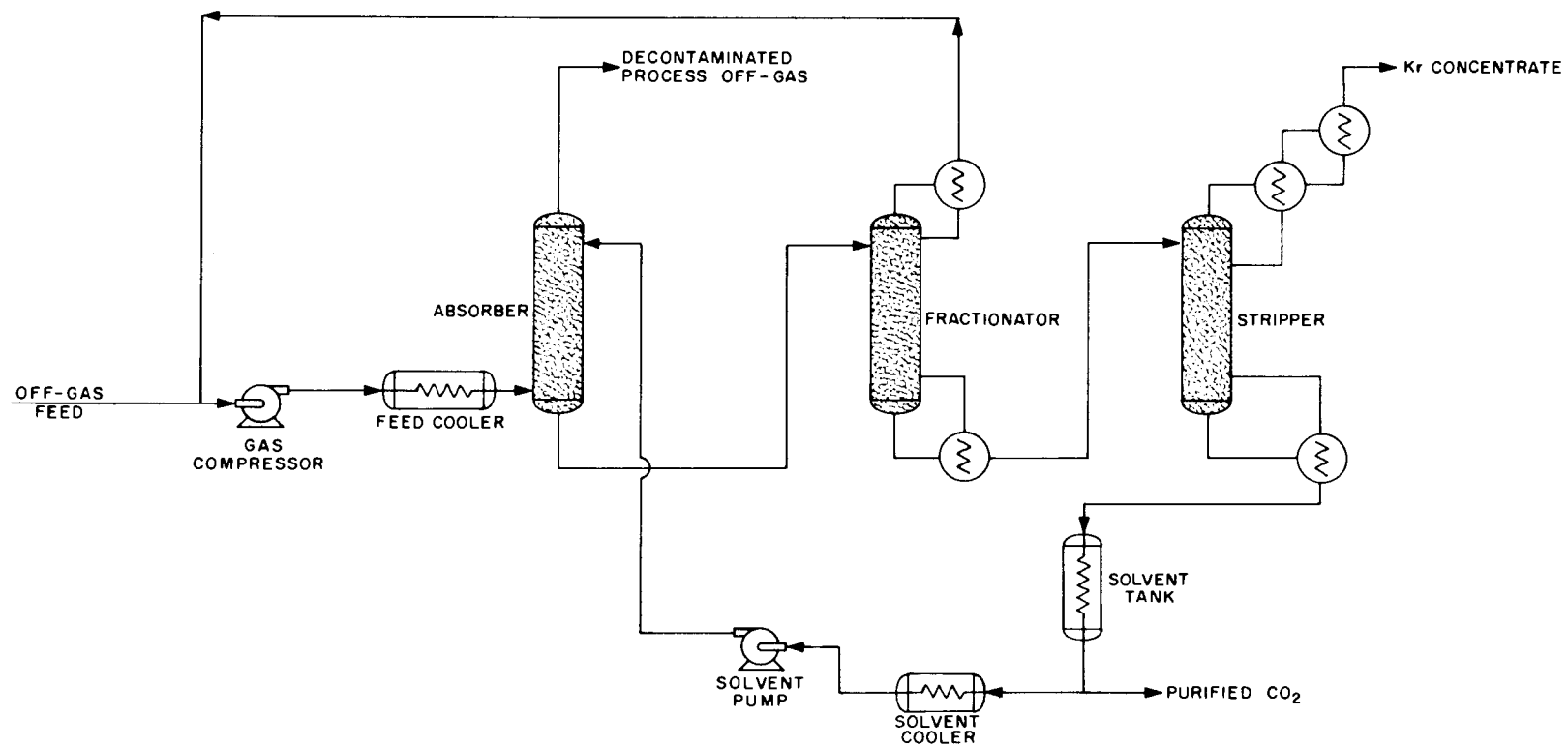


Fig. 15. Simplified Flowsheet for the KALC Process.

one-fifth of the  $\text{CO}_2$ ; about four-fifths is in the decontaminated liquid waste stream. The liquid waste stream can be vaporized and released to the environment, along with the gaseous waste stream.

Developmental work has proceeded along five lines: mathematical modeling, laboratory measurements of fundamental data, experimental engineering studies of individual process steps, integrated operation of a pilot plant (located at the ORGDP and adapted from their Freon absorption system), and development of the final concentration step. The calculational work has resulted in (1) an empirical equilibrium model for the  $\text{CO}_2\text{-O}_2\text{-Kr-Xe}$  system<sup>14</sup> to provide rapid but accurate information for data analysis and experimental planning, and (2) an advanced equilibrium stage model<sup>15</sup> for use in multicomponent, multicolumn calculations. The latter program represents thermodynamic properties of the  $\text{CO}_2\text{-O}_2\text{-N}_2\text{-CO-Kr-Xe}$  system accurately over the entire temperature, pressure, and concentration range of interest. Matrix algebra techniques are used to solve selected equilibrium stage configurations.

Laboratory studies were performed to determine accurately the solubilities of both Kr and Xe in liquid  $\text{CO}_2$ .<sup>16,17</sup> These fundamental properties are required for the calculations mentioned above, and also for treatment of the engineering data described below. These solubilities, expressed as separation factors, were measured by an in situ counting procedure developed for this study, utilizing  $^{85}\text{Kr}$  and  $^{133}\text{Xe}$  tracers. This procedure obviated the difficulties associated with the more traditional sampling techniques. The results are shown in Figs. 16 and 17, and are also of more general interest because they span the entire liquid range of  $\text{CO}_2$ .

The experimental engineering system is described completely elsewhere,<sup>18</sup> but a simplified equipment flowsheet is presented as Fig. 18. The system consists of two packed columns for gas-liquid contacting, plus associated support items including gas compressors, solvent pumps, condensers, heaters, and complete sampling and monitoring capabilities. Process cooling is achieved by means of two conventional evaporative-type refrigeration units. The  $^{85}\text{Kr}$  contents of various streams are measured via in-line beta detectors (Fig. 19) which were developed specifically for this application, and other

ORNL-DWG 72-6887R3

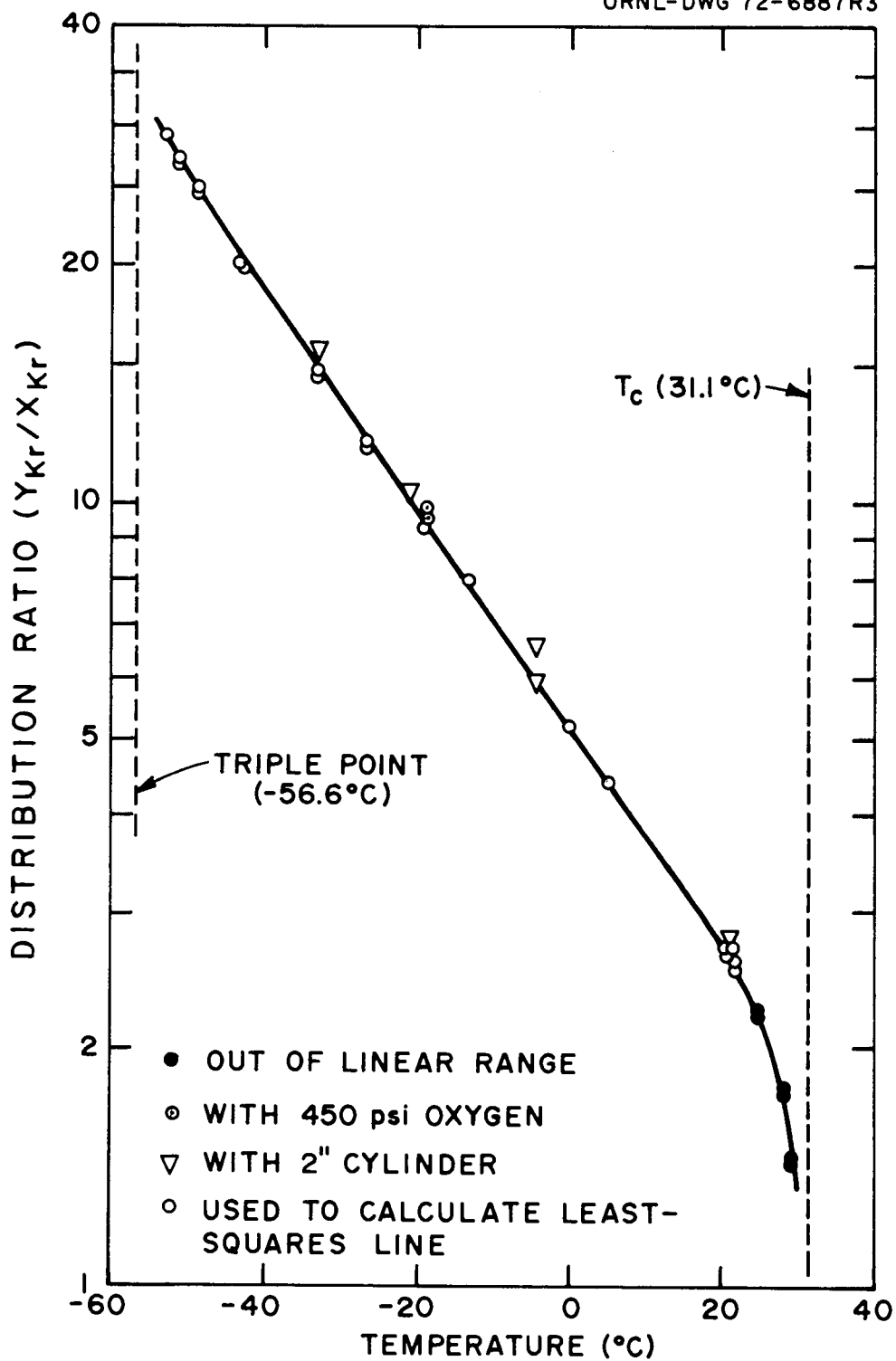


Fig. 16. Krypton Distribution Between Gaseous and Liquid  $CO_2$ .



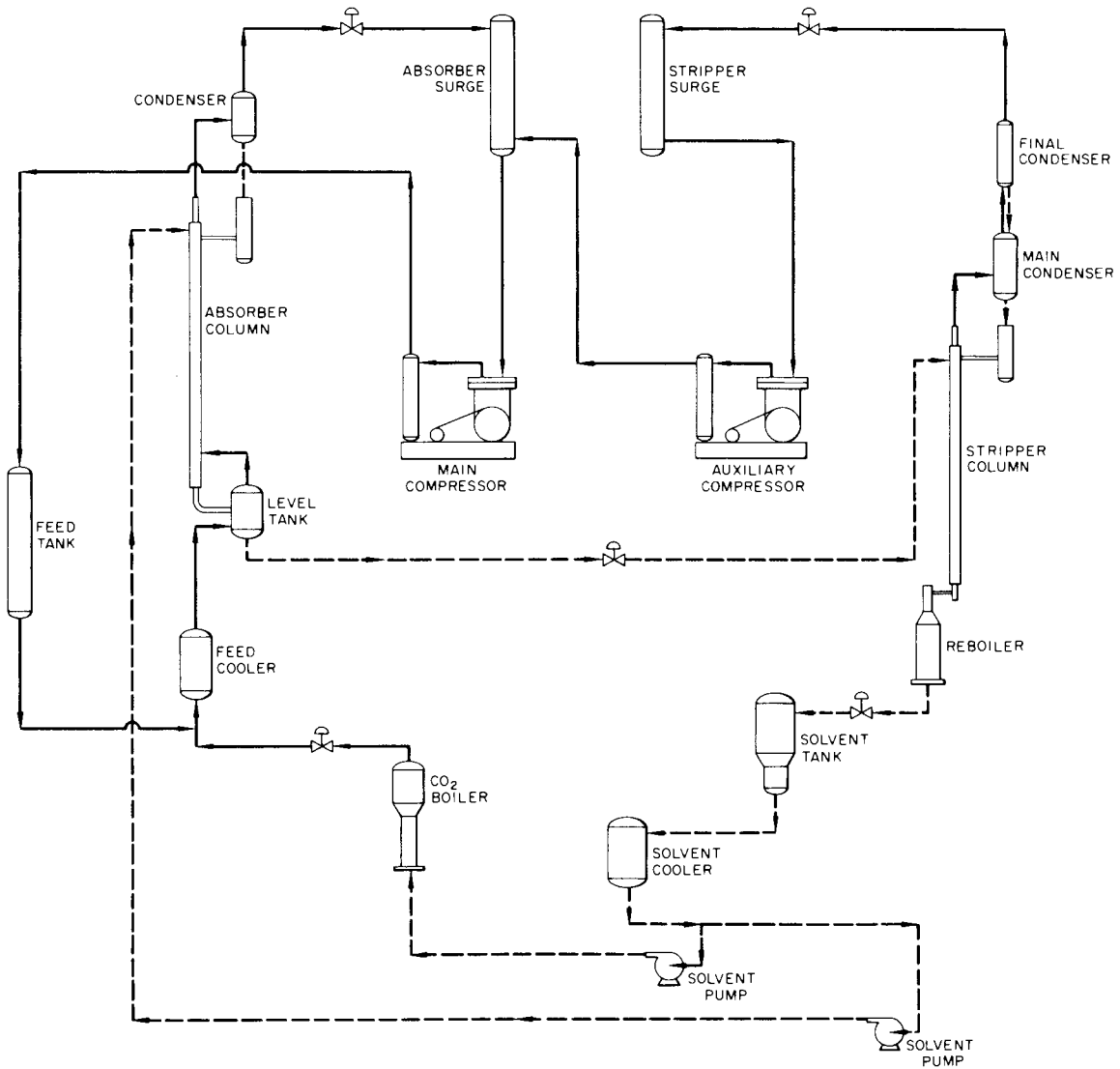


Fig. 18. Two-Column Experimental Engineering Facility to Study KALC Processes.

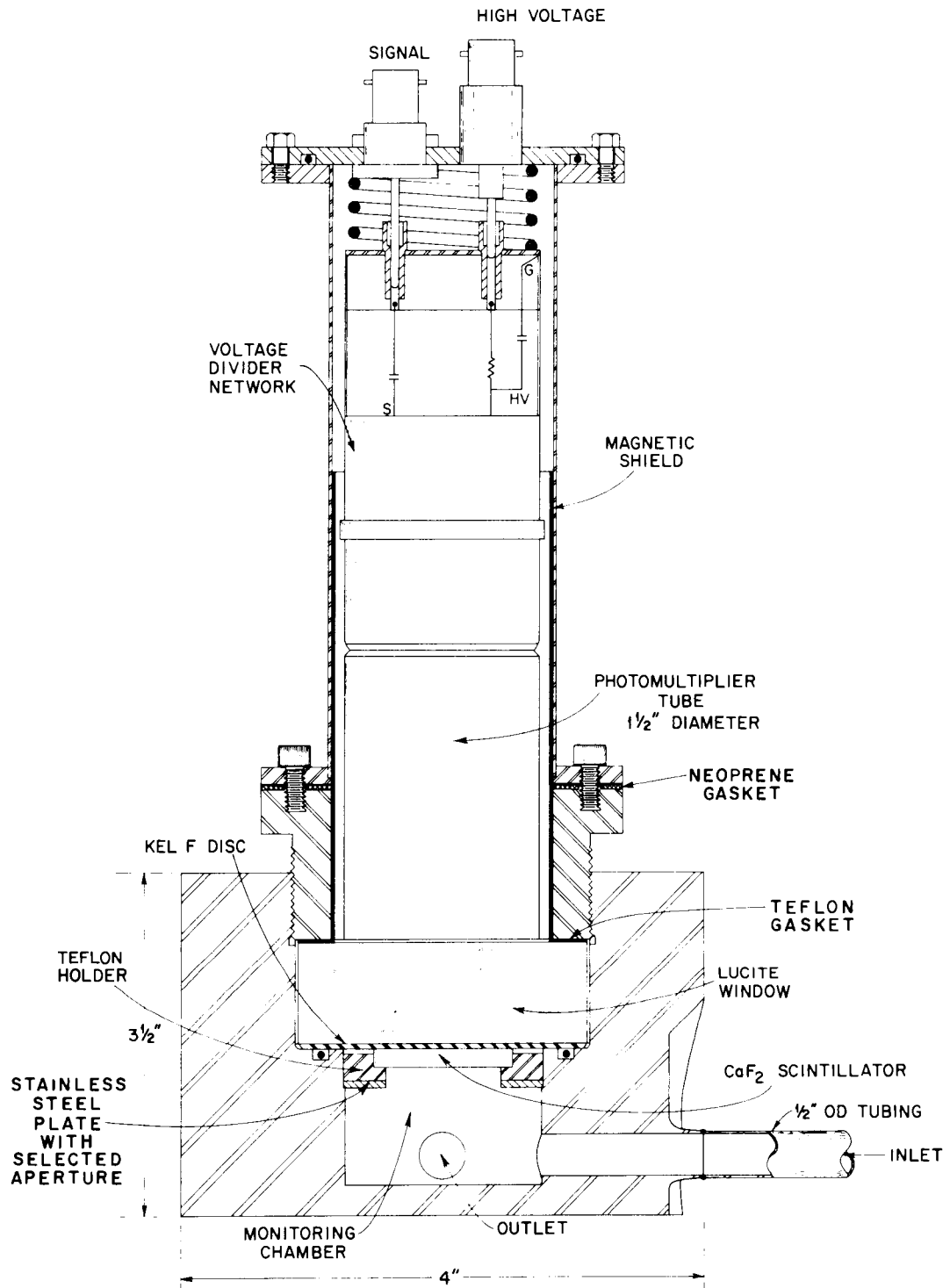


Fig. 19. High-Pressure Beta Scintillation Detector with Flow Cell.

components are determined by a sampling procedure using a capillary withdrawal technique.<sup>19</sup> Preliminary operation of the system began in March of 1974, and since that time, three experimental KALC campaigns have been completed. The first campaign was preliminary in nature and was completed in October of 1974. A primary goal for this campaign in addition to shakedown was the obtaining of column packing fluid dynamics. The flooding curve resulting from these and subsequent studies is presented in Fig. 20. The packing material used in these experiments is of the woven wire mesh cannister type (Goodloe Co.). The second campaign<sup>20</sup> was primarily concerned with mass transfer for absorption of krypton into liquid CO<sub>2</sub>. Some 30 experiments were conducted at conditions of 250 to 410 psig and -28° to -11°C. For column krypton decontamination factors of 100 to 10,000 a theoretical transfer unit height of about 0.4 ft was observed (see Fig. 21). Absorber column krypton decontamination factor as a function of the combined ratio of absorber liquid-to-vapor rates (L/V) and process krypton equilibrium values (K) is shown in Fig. 22. The results of the third campaign are being analyzed at this time.

The KALC system was tested in the ORGDP Pilot Plant in May and June 1974<sup>21</sup> and in a four-month campaign started in May 1975.<sup>22</sup> The first campaign served mainly as a shakedown of the equipment and a determination of the flooding rate of a packed column with CO<sub>2</sub>. The primary objective of the second campaign was to demonstrate simultaneous decontamination of a gas stream consisting of CO<sub>2</sub>-O<sub>2</sub> with respect to <sup>85</sup>Kr and concentration of the <sup>85</sup>Kr in the waste stream. The first campaign showed that generally satisfactory performance of the equipment was attained except for difficulty with the gas compressor and the refrigeration units. The shakedown tests also showed that additional instrumentation would be required to improve flow control and flexibility of operation. Flooding test data for the fractionator agreed very well with data obtained on a column of the same diameter in the ORNL facility, but the capacity was only about 50% of that predicted by the packing manufacturer.

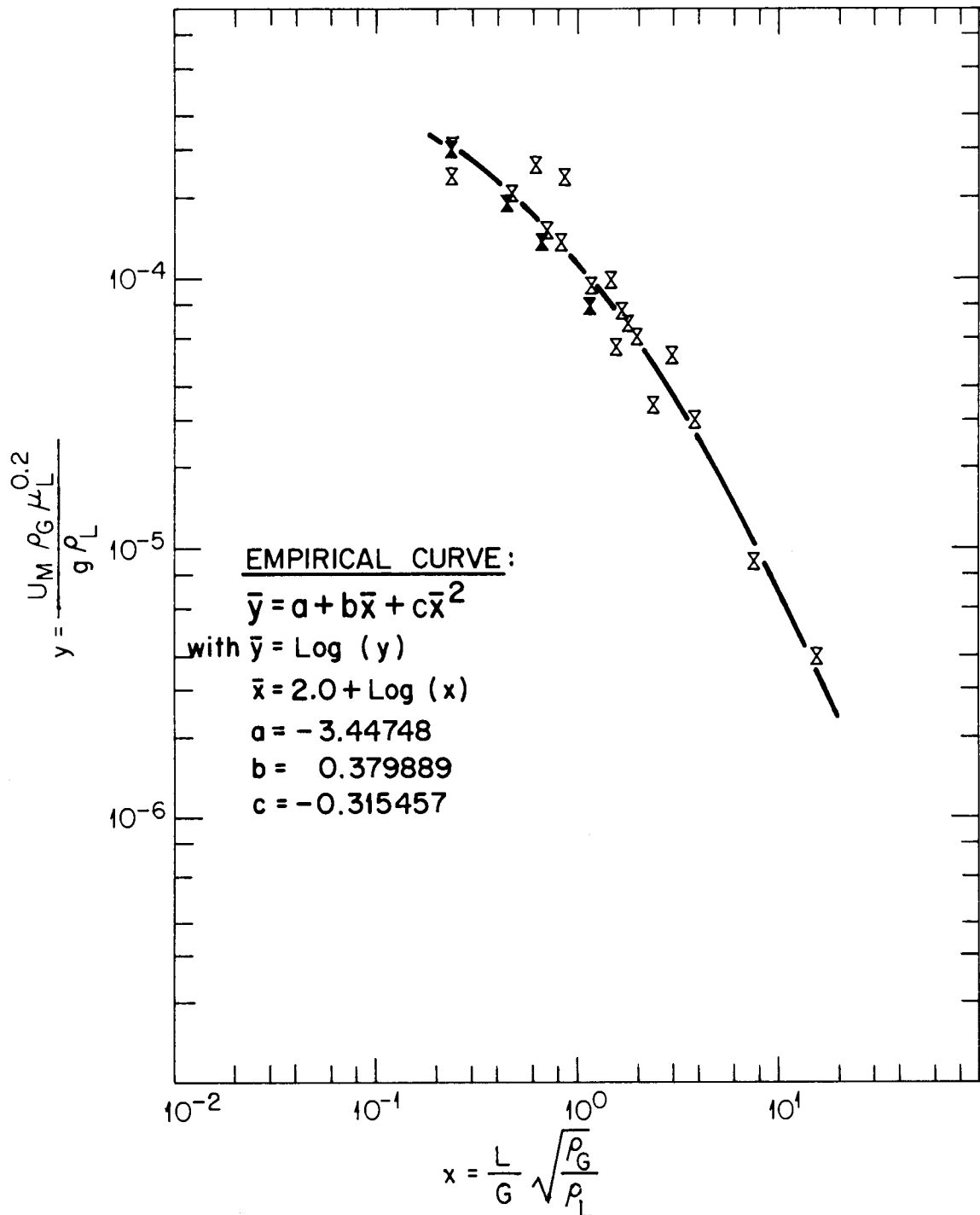


Fig. 20. Experimental Flooding Curve for KALC Systems.

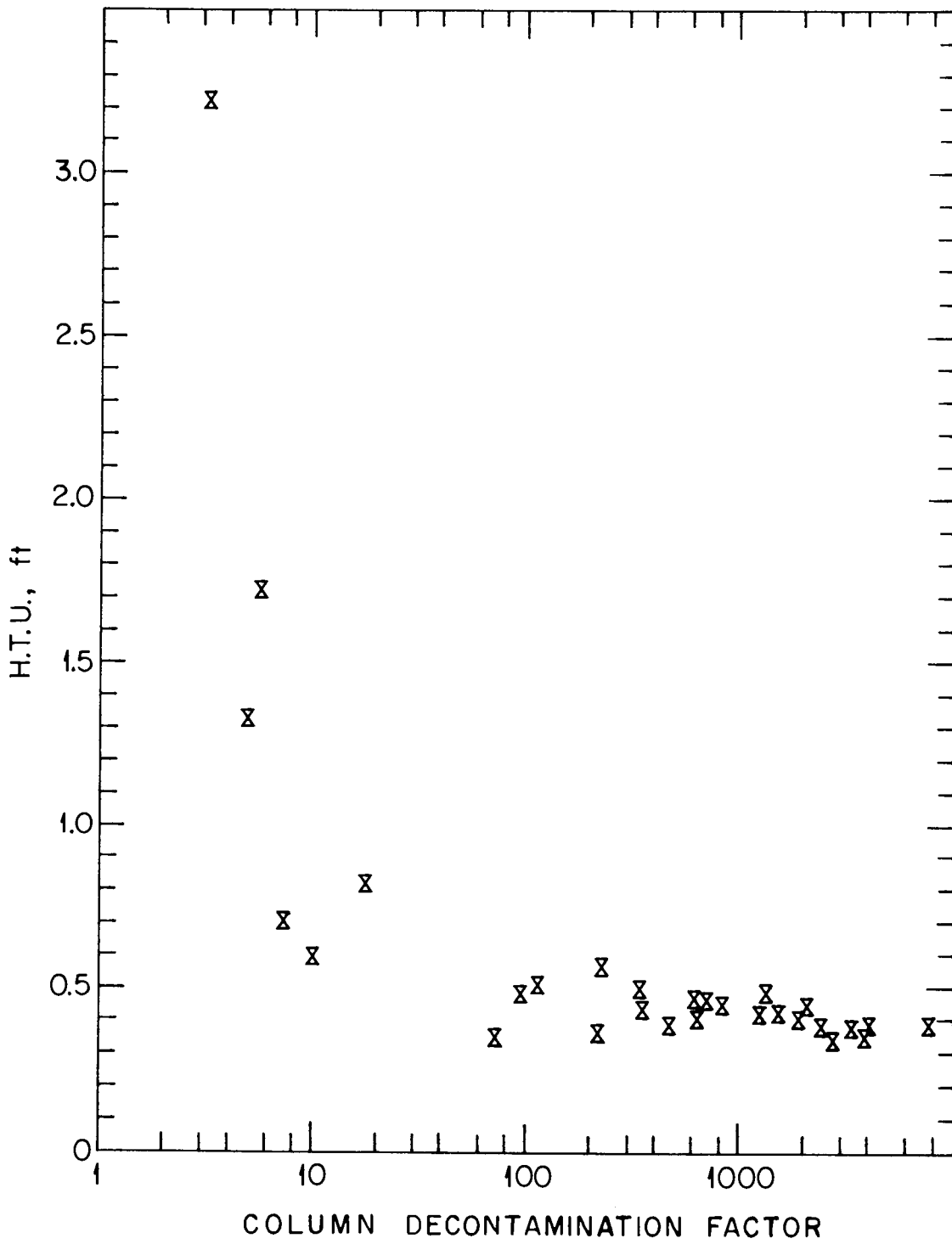


Fig. 21. Variation of Column HTU as a Function of Column DF.

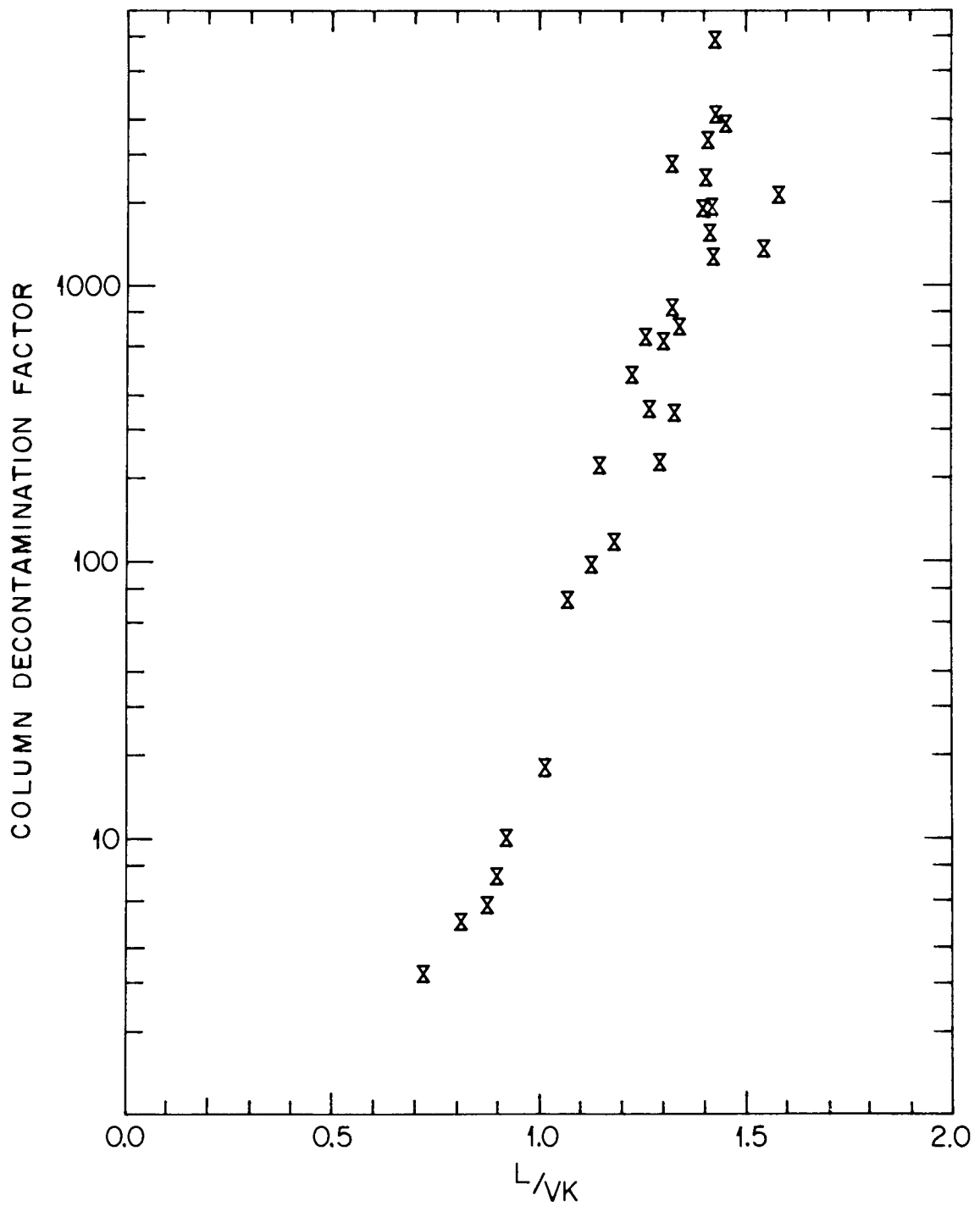


Fig. 22. Column Decontamination Factor as a Function of the Absorption Factor (L/VK).

The second campaign showed that operation is significantly improved with new instrumentation. The system control modes were adjusted to reduce flow oscillations, and runs were made with tracer  $^{85}\text{Kr}$ . Process decontamination factors greater than 100 were obtained and simultaneously, concentration factors greater than 1000 were obtained, thus exceeding the target objectives. Additional work is being carried out (in the Experimental Engineering facility) to optimize control modes, and future work will deal with the behavior of trace impurities.

Under optimum conditions for KALC, the Kr-rich product is still only  $\sim 1\%$  Kr, the balance being mostly  $\text{CO}_2$ , plus some Xe. Therefore, a final concentration step is required in order to minimize the storage volume. A process to do this via molecular sieves is being developed, in which  $\text{CO}_2$  is held back and only Kr (plus any  $\text{O}_2$  or  $\text{N}_2$ ) passes through.<sup>23</sup> The molecular sieve is regenerated by heating, and the  $\text{CO}_2$  driven off is recycled to KALC. This approach is feasible for the final Kr concentration step, but it is not practicable for the initial concentration from  $\sim 20$  ppm to  $\sim 1\%$ . Recent results indicate that this approach will work but, if it does not, a  $\text{CO}_2$  freeze-out method will be used.

#### Iodex Process Tests and System Studies

The Iodex process for iodine decontamination by nitric acid scrubbing is being developed for LMFBR application, where the iodine is in an air atmosphere.<sup>24</sup> For HTGR reprocessing, the iodine will be in a predominantly  $\text{CO}_2$  atmosphere. Three tests were conducted to test the Iodex process in such an atmosphere to establish feasibility for application to HTGR, should this ever be desired. Tests were run with a  $\text{CO}_2\text{-CH}_3\text{I}$  mixture and with a  $\text{CO}_2\text{-CO-I}_2$  mixture to simulate HTGR off-gas. In both tests, some air was also added to simulate the  $\text{O}_2/\text{N}_2$  content of HTGR off-gas. A control test was also run, using air- $\text{CH}_3\text{I}$ . The results are summarized in Table 11, and show that the Iodex process will work in a predominantly  $\text{CO}_2$  atmosphere containing some CO and  $\text{O}_2$ , typical of HTGR off-gas.<sup>25</sup>

Table 11. Tests of Iodex Process under HTGR conditions

	CH <sub>3</sub> I in Air (control)	CH <sub>3</sub> I in CO <sub>2</sub> -Air (7% air, 93% CO <sub>2</sub> )	I <sub>2</sub> in CO <sub>2</sub> -Air-CO (7% air, 1% CO, 92% CO <sub>2</sub> )
DF, Plate 1	6.3	5.9	6.4
2	4.0	3.6	5.5
3	2.7	3.0	4.4
4	3.0	2.8	4.9
5	2.9	3.1	4.0
6	2.4	2.5	1.6 <sup>a</sup>
7	3.1	3.3	6.5 <sup>a</sup>
Average <sup>b</sup>	3.3	3.4	4.4
DF, Column	4700	5000	33,000
DF, Condenser	13	10	3
DF, Overall	6 x 10 <sup>4</sup>	5 x 10 <sup>4</sup>	1 x 10 <sup>5</sup>

<sup>a</sup>Reflecting poor <sup>131</sup>I counting statistics for plate 7.

<sup>b</sup>Average DF = [(DF)<sub>1</sub> · (DF)<sub>2</sub> ··· (DF)<sub>7</sub>]<sup>1/7</sup>.

Spectrophotometric studies of the  $\text{CO}_2\text{-I}_2\text{-H}_2\text{O}$  system were carried out<sup>26,27</sup> originally under funding by the Division of Physical Research and later under the TU program. These studies have indicated that corrosion attack by iodine on stainless steel in a  $\text{CO}_2$  environment is greatly enhanced when traces of moisture are present. Distribution coefficients for  $\text{I}_2$  were determined in the absence of moisture (Table 12). The data also indicate that  $\text{CO}_2\cdot\text{H}_2\text{O}$  and  $\text{CO}_2\cdot 2\text{H}_2\text{O}$  association complexes are formed in the gas phase.

### III. ALTERNATE BURNER CONCEPT

The reference process for primary burning is fluidized-bed combustion, necessarily preceded by crushing of the fuel blocks to a size small enough to fluidize. Crushing is a major operation, with some undesirable side effects (dusting, gas release, some particle breakage), and fluidized bed burning inevitably generates large quantities of fines (which must be recycled). Because of these factors, whole-block burning is a potentially attractive alternative method, and experimental and theoretical studies of this approach were conducted. Although this work has been suspended within the Thorium Utilization Program, it led to a modified burning procedure -- so-called adiabatic burning -- which utilizes gas recycle and which has application to other non-fluidized bed burners (e.g., a chunk burner) and is, in fact, being actively studied as an engineering research project.

#### Experimental Demonstration of Feasibility

The experimental study<sup>28</sup> was carried out using one-sixth of a Fort St. Vrain fuel block; i.e., a prism 31 in. long and 7 in. across. Two views of the burner are shown in Figs. 23 and 24. The major objective of the study was to demonstrate an acceptable capacity without excessive temperatures or particle breakage, and this was accomplished. A graphite burning rate of 136 g/min was achieved, which is equivalent to the target rate for FB burners ( $30 \text{ kg/hr/ft}^2$ ). Maximum burning temperatures for a

Table 12. Distribution coefficients of  $I_2$  between  $CO_2$  liquid (l) and vapor (v)

Temperature ( $^{\circ}C$ )	$Dq (\pm 6\%)^a$
20	2.2
25	5.2
19	10.0
15	14.5
10	27.5
5	54.0
0	80.0
-10	135
-20	260
-26	320

<sup>a</sup>  
 Defined as:  $Dq = \left( \frac{\text{Specific Absorbance}_l}{\text{Specific Absorbance}} \right) \left( \frac{\rho}{\rho_l} \right)$   
 $= \frac{\text{mole fraction in liquid}}{\text{mole fraction in vapor}}$

where:

$$\text{specific absorbance} = \frac{I_2 \text{ absorbance at } 520 \text{ nm}}{\text{path length}}$$

and  $\rho = \text{density } CO_2$  .

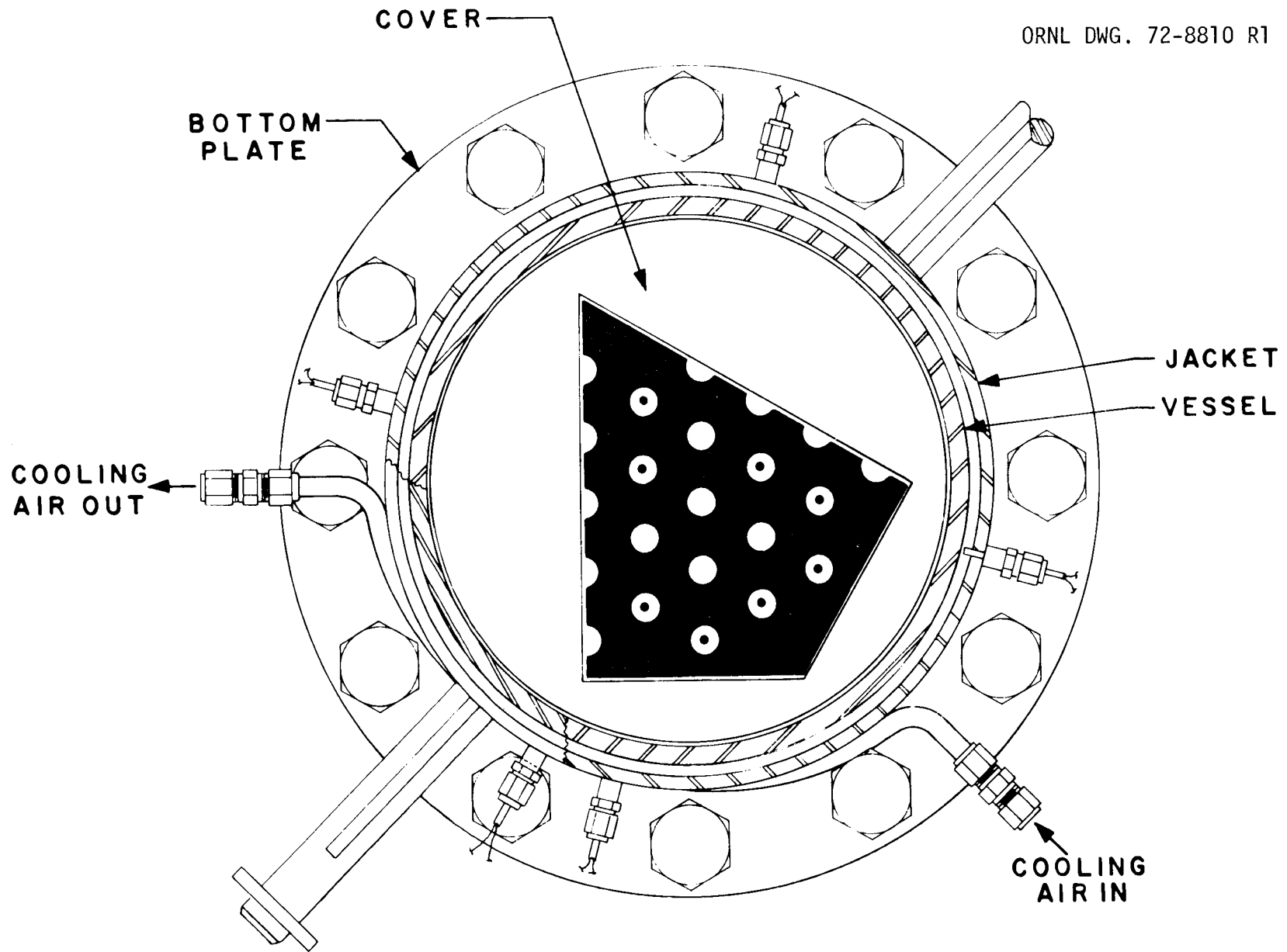


Fig. 23. Sectional View of Whole-Block Burner.

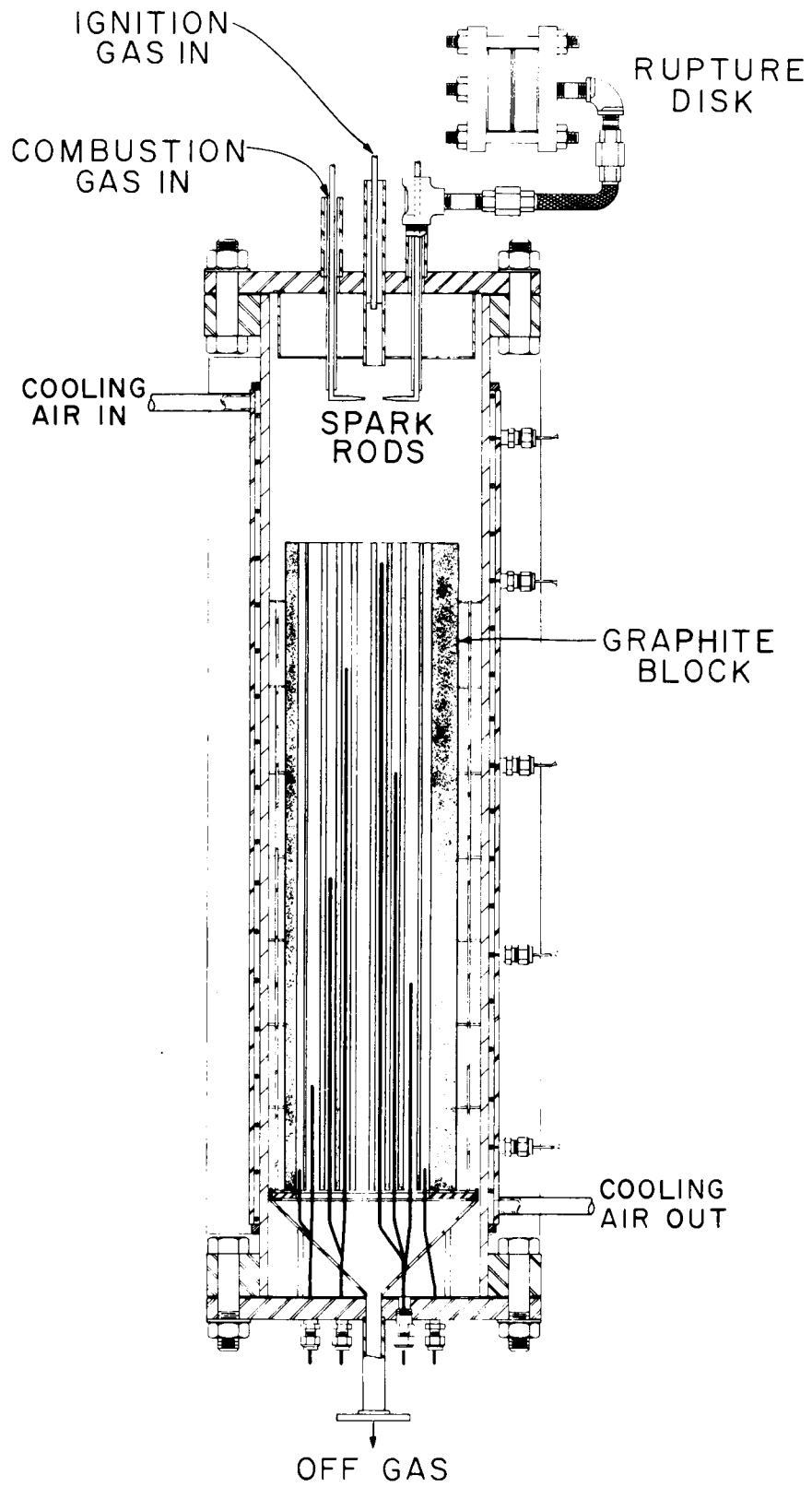


Fig. 24. Transverse View of Whole-Block Burner.

given run varied from 1050 to 1350°C, depending on conditions; corresponding wall temperatures were kept below 950° by means of external cooling. Coated particle breakage was determined to be less than 5%. The quantity of fines generated was very low: 1.7 wt % in one case and less than 0.5% for six other tests. At steady state, oxygen utilization was 99%. The ratio of CO/CO<sub>2</sub> in the off-gas was a function of temperature; below 1200°C there was no CO, and at 1350° the CO ranged between 15 and 25%. These results prompted the paper studies described below.

#### Evaluation and Theoretical Studies

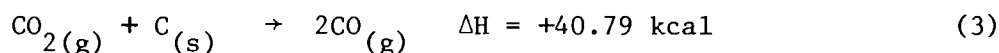
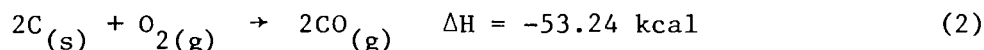
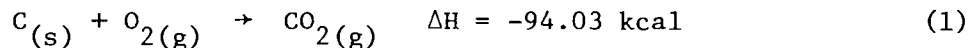
An economic and technical comparative study<sup>29</sup> was made of fluidized-bed burning and whole-block burning for performing the primary burning step in HTGR fuel reprocessing. For each method, the ancillary equipment for heat removal and the fuel and ash handling were considered; crushing was also included in the case of fluidized-bed burning. The scale of primary burning was that of a reprocessing plant handling the spent fuel from ~ 50,000-MW(e) HTGR generating capacity. Preliminary designs were prepared for the major equipment components and/or modules in canyons equipped with the necessary remote maintenance features. Cost estimates were prepared for the equipment items using a fractional cost factor for multiple modules. The cost of the building associated with the primary burning step was estimated using the volume of concrete in the heavily shielded canyons and the area of the operating corridors adjacent to or above the canyons. The capital cost of primary burning was estimated at about \$100 million, with no over-riding differences between fluidized-bed and whole-block burning. However, the layout of the various canyons suggested that a modular head-end plant with add-on capability is more easily obtainable with the whole-block burner than with the fluidized-bed burner.

A theoretical study was made of the so-called "adiabatic" burner, wherein most of the heat is removed from the system downstream of the burner via a separate heat exchanger.<sup>30</sup> Burner conditions are controlled by appropriate recycle of burner off-gas, utilizing the endothermic reaction,  $\text{CO}_2 + \text{C} \rightarrow 2\text{CO}$ , and high gas velocities. A simplified model was

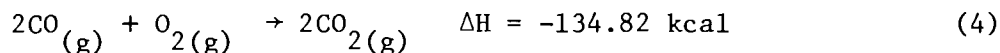
selected and computer programs were written to calculate gas compositions and temperatures throughout the burner. Complete utilization of  $O_2$  or low concentrations of  $O_2$  in the exit gas depend on graphite temperatures that are sufficiently high to produce CO, which reacts with  $O_2$  in the bulk gas. It does not appear practical to operate under conditions that promote both high utilization of  $O_2$  and low CO concentration in the exit gas. Instead, the burner conditions should be chosen to clearly favor moderate concentrations of either  $O_2$  or CO in the exit gas. Moderate concentrations of  $O_2$  in the exit gas would allow lower graphite temperatures and would probably give the desired burning rates for three axially aligned blocks. Moderate concentrations of CO in the exit gas would ensure high burner capacities but would result in higher temperatures and more complex burner control behavior. A suggested flowsheet is shown schematically in Fig. 25.

#### Gas Recycle Burner Studies

Currently, experimental work on the "adiabatic" or gas-recycle concept, as suggested by the theoretical study, is being carried out under funding by the Division of Physical Research. This work focuses on control modes and recycle of off-gas.<sup>31,32</sup> Results to date have verified the basic conclusions of the theoretical study, and have also achieved high burning rates. The reactions occurring in graphite oxidation are:



In addition to these, a gas-phase reaction occurs:



Reactions (1) and (2) are sufficiently rapid so that combustion of graphite is controlled by  $O_2$  diffusion at temperatures of interest (1600°C maximum). Since both reactions are exothermic, the process is self-sustaining once the ignition temperature (750°C) is reached. A large

ORNL DWG 74-1302

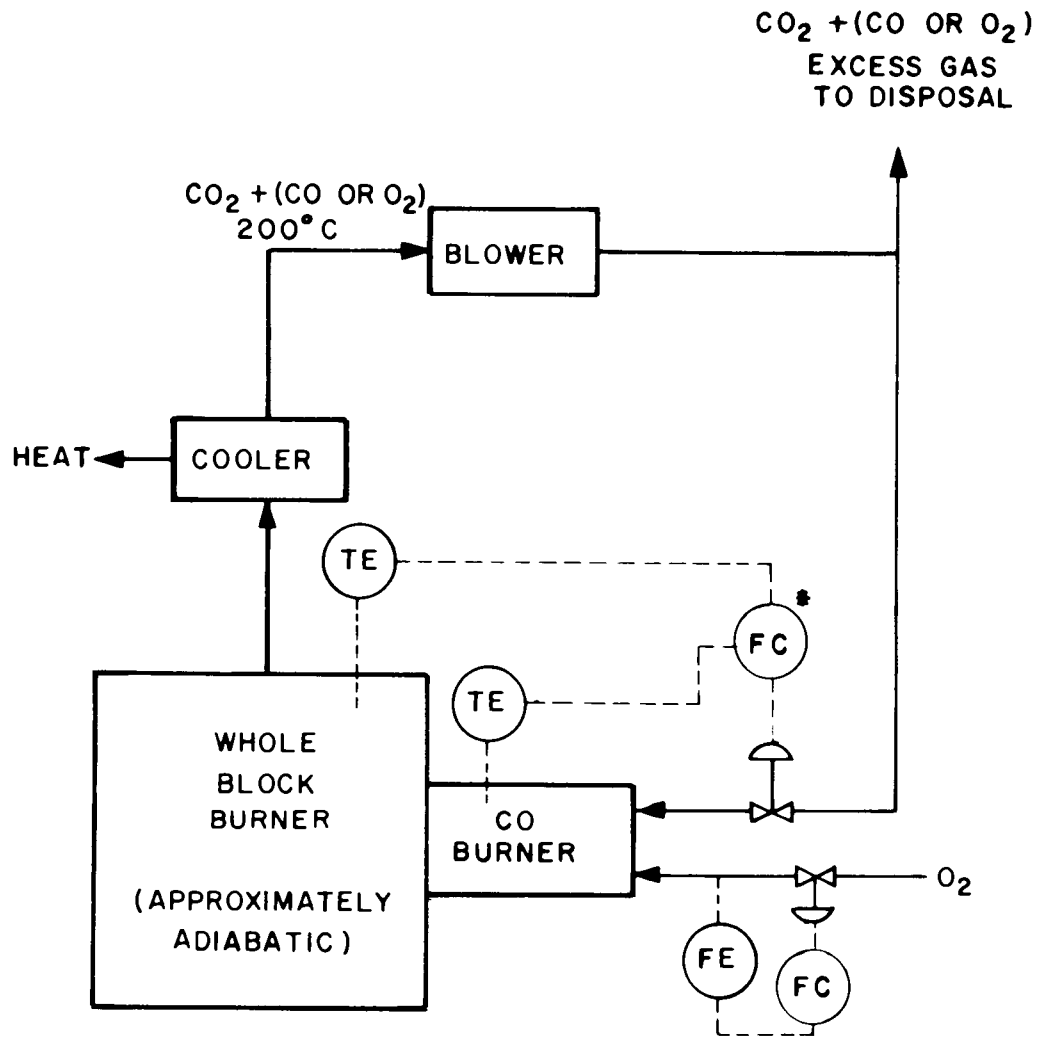


Fig. 25. Recommended Flowsheet for an Adiabatic Whole-Block Burner.

amount of heat is released which is partially utilized by reaction (3) at graphite temperatures above 1300°C. Although CO production by reaction (2) is highly favored at all temperatures which give acceptable burn rates, CO is quickly oxidized to CO<sub>2</sub> as it counter-diffuses with O<sub>2</sub> in the gas boundary layer. As a result, significant levels of CO in the flue gas are not encountered unless the O<sub>2</sub> content is near zero. Extremely high burning temperatures (above 1450°C) will result in CO in the exit gas caused by an increased rate of reaction (3), and burnup of the available oxygen by reaction (4). Although reaction (3) will prevent extremely high graphite temperatures, it is not sufficiently rapid to maintain gas temperatures at the desired level (1000°C). Therefore, recycle is used to increase the gas flow rate through the burner and to remove the excess heat. Molar recycle rates will range from three to eight times the oxygen flow rate, depending on the burn rates desired.

Equipment was designed and constructed to test the predicted results for a recycle burner. The graphite burner (Fig. 26) is a 14-in.-diam pipe, approximately 58 in. long, and is fabricated from type 347 stainless steel. The upper section, 35 in. long, contains the burn zone and is externally insulated. Solid graphite rods, 24 in. long and 1 to 1-1/2 in. diam, are heated by electrical clamshell heaters to ignition temperature (750°C). The firebrick liner and insulation prevent high burner wall temperatures and reduce heat losses to approximately 5%. The gas temperature at the burner exit is normally 600 to 1100°C. Cooled gases are injected at the top of the cooling chamber to reduce the gas temperature to approximately 500°C. The cooling coil is 3/8-in. stainless steel, spiral-wound into eight flat coils to obtain cross-flow heat transfer. The coil contains approximately 100 ft of tubing and is water-cooled. The graphite and clamshell heaters rest on firebrick supported by a water-cooled stainless steel pipe. Flue gas temperatures at the cooling zone exit are about 150 to 250°C. The overall equipment layout (Fig. 27) includes a cyclone, filters, and heat exchangers, as well as rotameters and CO, CO<sub>2</sub>, and O<sub>2</sub> in-line analyzers.

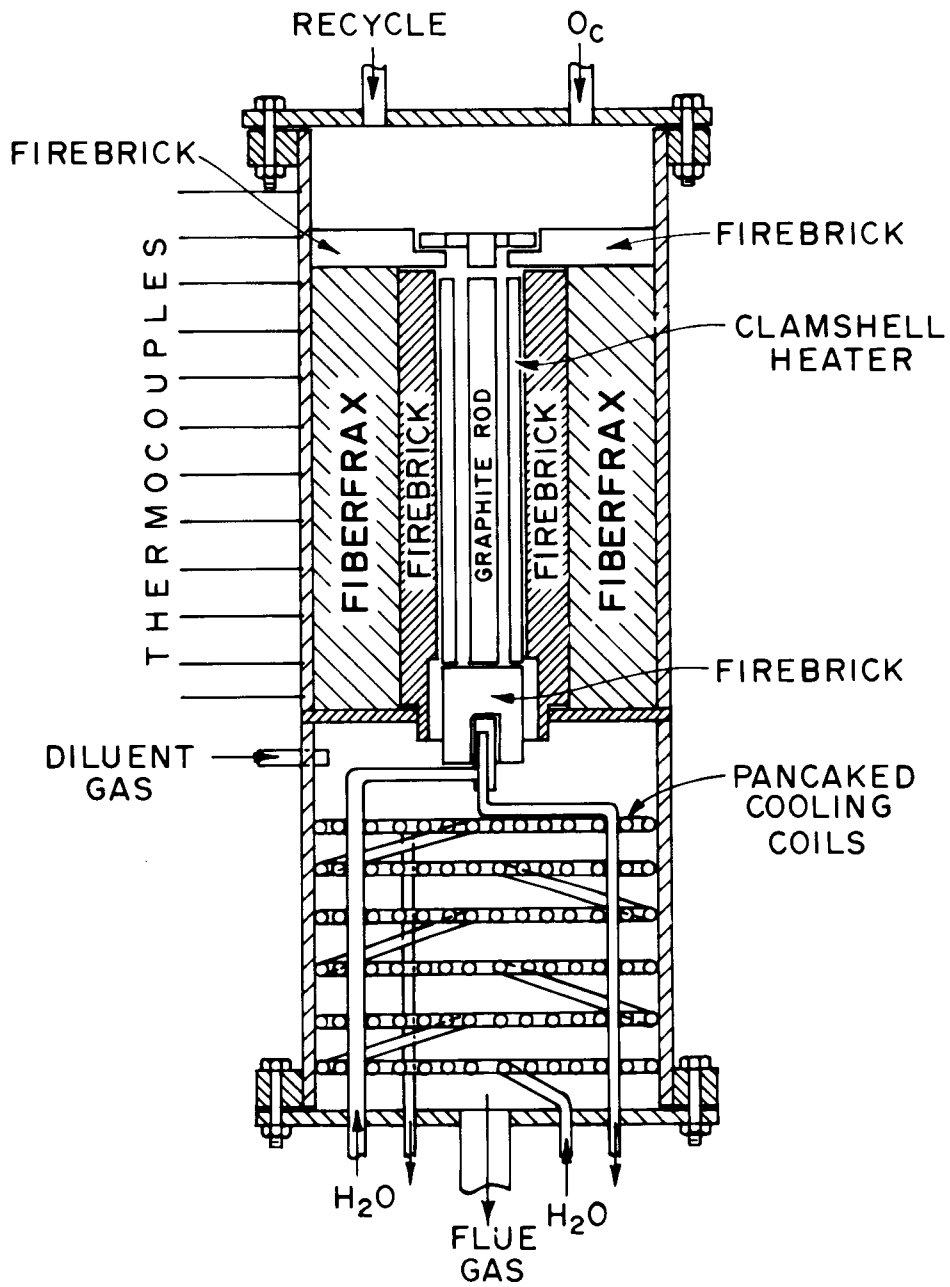


Fig. 26. Adiabatic Graphite Burner.

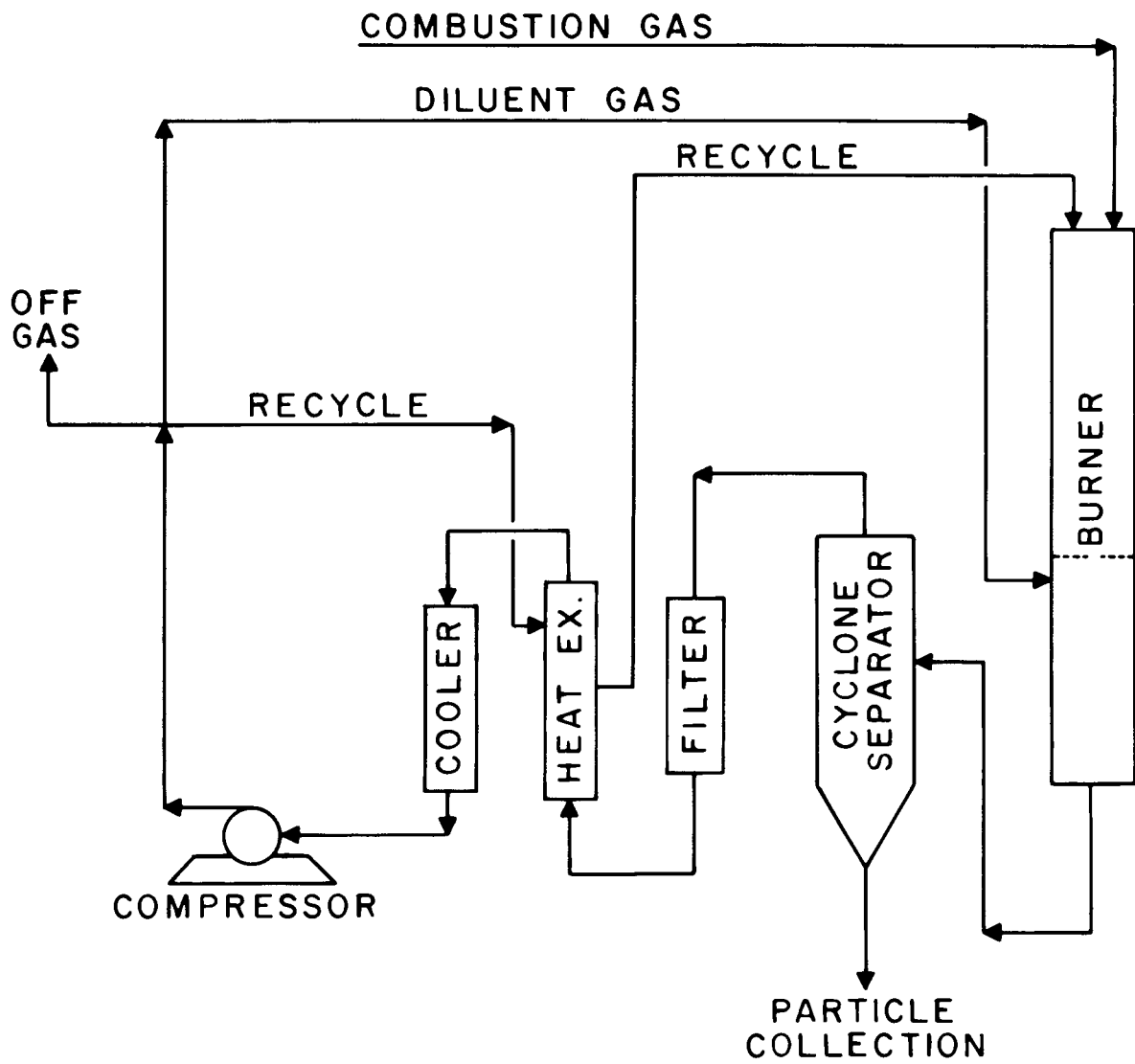


Fig. 27. Equipment Flowsheet for Adiabatic Burning Studies.

Several graphite rods were burned to determine the important variables. Previous studies<sup>33</sup> of carbon rod combustion suggest that the oxidation is mass transfer controlled at velocities as high as 165 m/sec. Our investigations with graphite rods agree with this. Gas velocities up to 12 m/sec have been studied, and reaction rates increase with gas flow rate. No dependence of reaction rate on graphite temperature has been observed in the temperature range studied (1000°C - 1200°C). Typically, a "spike" in CO concentration of a few percent is observed in the product gas immediately after startup. The CO concentration then decreases to 1 or 2 percent and remains at a low value throughout the burn. The CO<sub>2</sub> concentration rises quickly, then gradually declines as less area is available for burning. With this burner, exit oxygen concentrations significantly below 15% have not been obtained. A longer burning zone is required to obtain better oxygen utilization in the recycle mode; the theoretical study showed that 3 m was required. Experimental burning rates up to 2 g-moles/min were obtained, which is equivalent to about 50 kg C/hr/ft<sup>2</sup>. To establish the feasibility of graphite temperature control by variation of recycle rate, a temperature control loop was installed. The exit gas temperature was sensed, and the recycle gas flow rate was varied to hold the temperature at the desired value. Isothermal control was achieved within five minutes. Fines production has been < 2%. Future work will deal with correlation of the theoretical model with observed results, control of longitudinal burning rate, and verification of the control method.

#### IV. SOLVENT EXTRACTION

##### Computer Modeling

The SEPHIS (Solvent Extraction Processes Having Interacting Solutes) computer program, which was developed to calculate the concentrations of the various components in the solvent extraction of U, Pu, and nitric acid by tributyl phosphate (TBP), was adapted to the Th extraction system. The SEPHIS program was originally developed for the calculation of the transient concentrations of uranium, plutonium, and nitric acid in

multi-staged solvent extraction systems using 15% TBP as the extractant.<sup>34</sup> This program was modified for use with the conventional Purex system and expanded to calculate a full partitioning cycle.<sup>35</sup> Recently, this SEPHIS-Purex program was improved.<sup>36</sup>

We have now modified the SEPHIS program to the Acid Thorex flowsheet. The pseudo-mass-action "constants" for thorium, uranium, and nitric acid are defined by the following equations:

$$K'_U = \frac{[\text{UO}_2(\text{NO}_3)_2 \cdot 2 \text{ TBP}]}{[\text{UO}_2^{2+}][\text{NO}_3^-]^2[\text{TBP}]^2}$$

$$K'_{\text{Th}} = \frac{[\text{Th}(\text{NO}_3)_4 \cdot 3 \text{ TBP}]}{[\text{Th}^{4+}][\text{NO}_3^-]^4[\text{TBP}]^3}$$

$$K'_H = \frac{[\text{HNO}_3 \cdot \text{TBP}]}{[\text{H}^+][\text{NO}_3^-][\text{TBP}]}$$

Because of the changes in the activity coefficient ratios with composition, the  $K'$  values are not constant and were calculated from the empirical equations

$$K'_U = C_1 + C_2\mu + C_3\mu^2 + C_4\mu^3$$

$$K'_{\text{Th}} = C_5 + C_6\mu + C_7\mu^2 + C_8\mu^3$$

$$K'_H = C_9 + C_{10}\mu + C_{11}\mu^2 + C_{12}\mu^3,$$

where the ionic strength was defined as

$$\mu = [\text{H}^+] + 3[\text{UO}_2^{2+}] + 10[\text{Th}^{4+}]$$

The 12 empirical constants were determined by least-squares fitting to minimize the difference between the calculated and observed organic-phase concentrations. The distribution coefficients and free TBP concentrations

were then calculated using the pseudo-mass-action values. It was found necessary to calculate separate sets of constants for the best distribution coefficient determinations of each extractable species (i.e., thorium, uranium, and nitric acid); therefore, 36 constants were used.

The accepted complex for the extracted thorium is  $\text{Th}(\text{NO}_3)_4 \cdot 2\text{TBP}$ .<sup>37</sup> However, a satisfactory fit to experimental data could not be obtained using this complex. The  $\text{Th}(\text{NO}_3)_4 \cdot 3\text{TBP}$  complex used in the program agrees with previously determined fits at this site.<sup>38</sup>

Calculations made by the computer code have been compared with data from laboratory countercurrent batch extraction experiments (Table 13). Similar agreements between calculated and experimental values have been found for the partitioning or costrip steps of the system.

The SEPHIS-Thorex program was used as an aid in determining the HETS of pulse columns for thorium extraction and in preparing the design of a proposed HTGR fuel recovery plant. Other parameters pertinent to the SEPHIS-Thorex code but which have not been completed include the effects of TBP concentration, temperature, and third-phase formation.

#### Experimental Tests; Sparging Effects

In conjunction with hot-cell burning studies, batch shakeout extraction tests were performed. The results (Fig. 28) show that Pu tends to follow Th, even in acid-deficient feed. This result was contrary to expected behavior and still needs to be verified, but is plausible in view of the high nitrate concentrations in these solutions.

Related to solvent extraction is the radioactivity of the purified product uranyl ( $^{233}\text{U}$ ) nitrate, which also contains  $^{232}\text{U}$  and its daughters. These give rise to the penetrating activity which necessitates gamma shielding, and they also contribute to the overall alpha activity. The gamma activity can be reduced significantly for a useful period of time by providing additional cleanup of the  $^{232}\text{U}$  daughters via ion exchange (Fig. 29). The benefits of sparging to remove  $^{220}\text{Rn}$ , while providing a large reduction in gamma activity after several days of continuous sparging,

Table 13. Experimental and calculated results for  
Acid Thorex solvent extraction system

Flowsheet Conditions

Feed: 278 g/l Th, 17.6 g/l U, 0.21 M AD, 1 volume

Scrub No. 1: H<sub>2</sub>O, 0.8 volume at stage 6S.

Scrub No. 2: 5 M HNO<sub>3</sub>, 0.2 volume at stage 3S.

Salting acid: 13 M HNO<sub>3</sub>, 0.5 volume at stage 4E.

Solvent: 30% TBP-NDD, 7 volumes at stage 5E.

Stage	Aqueous Phase		Organic Phase	
	Experimental	Calculated	Experimental	Calculated
<u>Thorium (g/l)</u>				
6S	85.9	86.0	40.2	39.5
5S		95.7		49.3
4S	103	90.9	50.4	50.5
3S		85.4		49.8
2S	90.6	96.9	52.6	51.6
1S		109		53.2
1E	126	117	55.8	55.1
2E		40.9		33.2
3E	11.6	8.2	11.6	11.6
4E		0.50		2.3
5E	0.27	0.09	0.27	0.15
<u>Uranium (g/l)</u>				
6S	0.31	0.32	2.64	2.51
5S		0.30		2.57
4S	0.28	0.28	2.69	2.55
3S		0.26		2.53
2S	0.28	0.27	2.74	2.55
1S		0.28		2.55
1E	0.30	0.29	2.54	2.55
2E		0.016		0.08
3E	0.0001	0.0016	0.002	0.004
4E		2 x 10 <sup>-5</sup>		0.0005
5E	< 0.0001	3 x 10 <sup>-6</sup>	0.0005	7 x 10 <sup>-6</sup>
<u>Acid (M)</u>				
6S	0.42	0.46	0.07	0.08
5S		0.88		0.13
4S	1.26	1.31	0.19	0.18
3S		1.81		0.23
2S	1.60	1.60	0.23	0.19
1S		1.38		0.16
1E	1.03	1.10	0.13	0.13
2E		1.85		0.28
3E	2.36	4.65	0.50	0.49
4E		4.40		0.72
5E	1.85	2.71	0.47	0.60

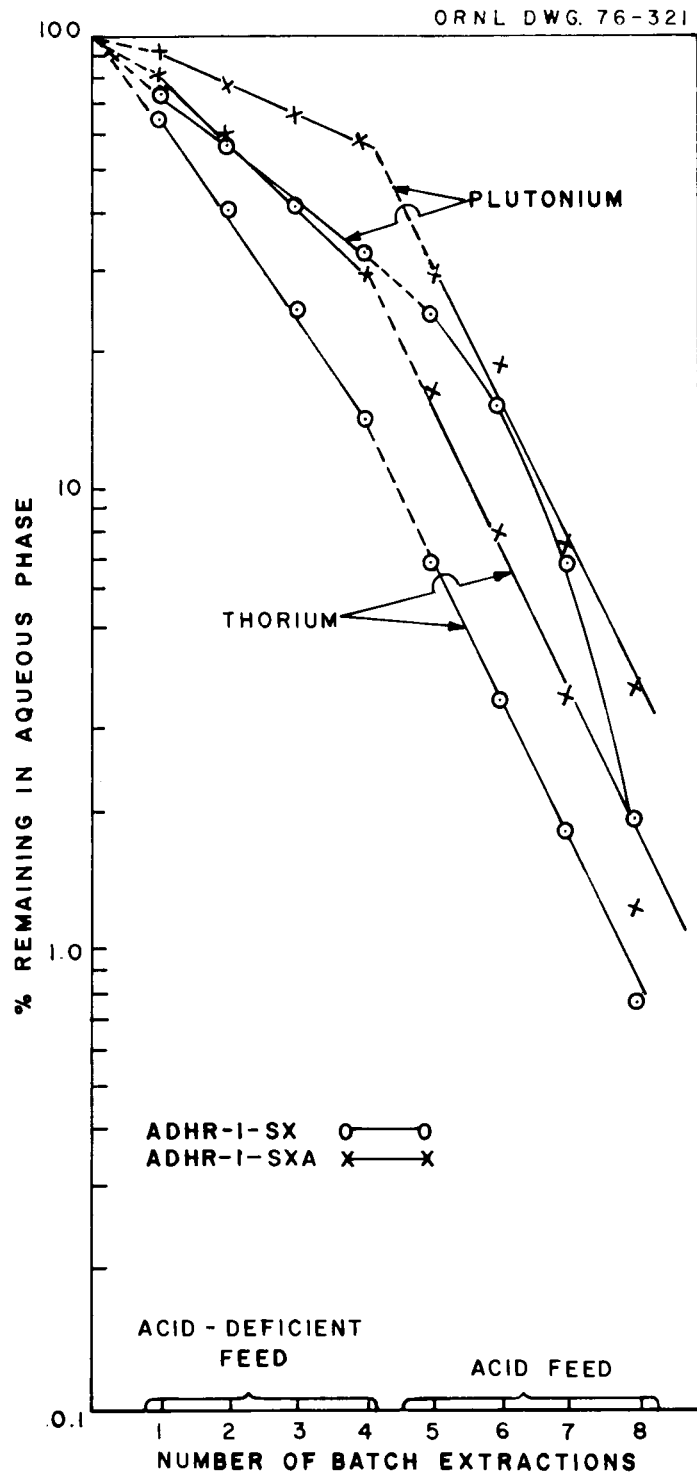


Fig. 28. Extraction of RTE-2-3 Fuel Solution in Hot Cell Experiments.

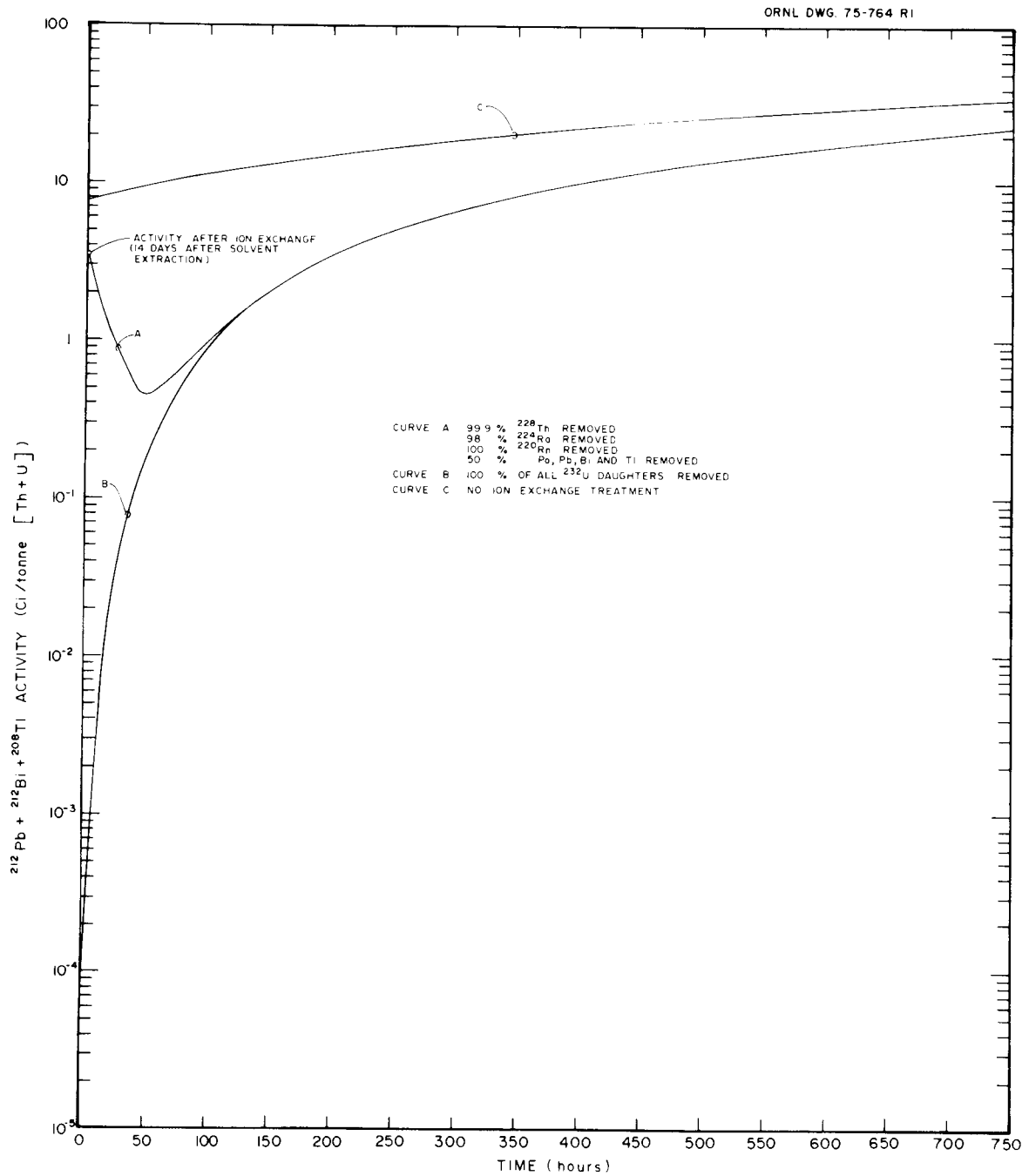


Fig. 29. Reduction in Activity of  $^{232}\text{U}$  Daughters by Ion Exchange Cleanup of  $\text{UO}_2(\text{NO}_3)_2$  Solution.

disappear very quickly after sparging ceases (Fig. 30).<sup>39,40</sup> This is because removal is governed by the half-life of the  $^{212}\text{Pb}$  decay (10.6 hr), while regrowth of the  $^{212}\text{Pb}$  is governed by the half-life of the  $^{220}\text{Rn}$  itself (55 sec); the  $^{220}\text{Rn}$  precursors,  $^{232}\text{U} \rightarrow ^{228}\text{Th} \rightarrow ^{224}\text{Ra}$ , are not affected by sparging.

## V. WASTE PROCESSING AND ISOLATION

Waste streams of various forms are produced at different process steps in HTGR fuel reprocessing. The major sources of these wastes may be grouped into four areas -- head-end processing, solvent extraction, off-gas cleanup, and miscellaneous sources. The individual sources are shown in Table 14 under these four major groups.<sup>41,42</sup> Essentially all the waste streams resulting from head-end processing are in solid forms while those discharged from the solvent extraction system are practically all liquids. Solid, liquid, and gaseous wastes are produced in the off-gas cleanup operation.

### Characterization Studies

Most of the waste streams are unique to HTGR fuel reprocessing, although those from the solvent extraction system and from the plant facilities are not very much different from wastes discharged from an LWR fuel reprocessing plant. The liquid high-level wastes, however, are somewhat different from the corresponding wastes in LWR fuel reprocessing in that they contain Th, Al, and a different fission product cation spectrum plus fluorides that were introduced to facilitate dissolution of thorium. Thus, there is a requirement to convert fluorides into a stable form before solidification of the waste at high temperatures. Solid waste streams include waste fissile particles (from 25W fuel elements), SiC hulls, and perhaps clinkers. Selection of specific processing methods (e.g., whether to separate actinides from fission products or not) for these wastes may well be governed largely by future Federal regulations and other non-economic factors. A gaseous waste,  $^{14}\text{CO}_2$ , may have to be converted into a form acceptable for isolation.

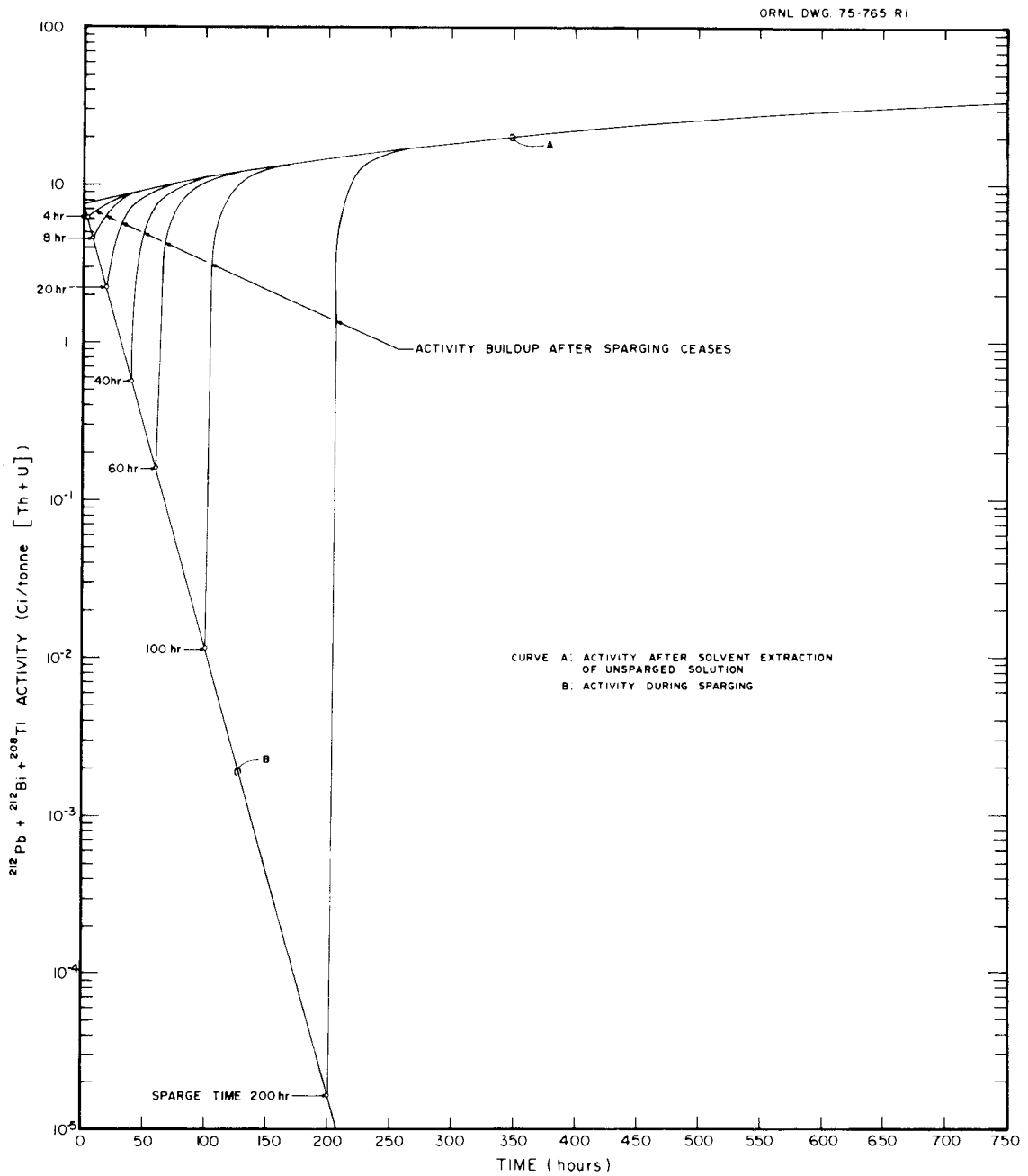


Fig. 30. Effect of Sparging  $\text{UO}_2(\text{NO}_3)_2$  Solution to Reduce Activity of the  $^{232}\text{U}$  Decay Chain.

Table 14. Sources and Estimated Flow Rates of Waste Streams from HTGR Fuel Reprocessing Plant

[Basis: 20,000 Fuel Elements/yr; 58% 25R, 39% 23R, 3% 25W]

Stream No.	Source (Subsystem)	Waste Form	Approx. Quantities per yr (Est.)	Probable Key Radionuclides Present (Est. Amt/yr)
<u>Head-End Processing System</u>				
H-1	Primary and secondary burners	Semi-volatile nuclides, particulates	110 kg, 10 MCi; particulates incl. in H-3	Fission products (e.g., Zr, Nb, Ru, Sb, Cs, Ce, etc.), actinides
H-2	Primary and secondary burners	Clinkers	0-6 MT <sup>a</sup>	Fission products, actinides
H-3	Crushers, hoppers, classifier	Particulates	12 MT	Fission products, actinides
H-4	Fissile particle canning station	Fissile particles (from 25W blocks)	4 MT	Actinides (U = 1.3 MT; 170 Ci); fission products (1 MT; 62 MCi)
H-5	Particle dissolver, centrifuge	SiC hulls, insol. residues (incl. noble metals)	20 MT	Actinides (5 kg, 4300 Ci); fission products (1.2 MT; 70 MCi) (esp. noble metals)
<u>Solvent Extraction System</u>				
S-1	Feed preparation	Steam stripper overhead	1,100,000 gal <sup>b</sup> (solid content $\approx$ 0.5-1% wt)	I, Ru
S-6	Uranium salvage	Evaporator condensate		I, Ru
S-7	First and second cycle extraction	Carbonate wash solution		Zr, Nb, Ru, Rh, I
S-2	Feed preparation	Insol. residue	1-3 MT	Zr, Nb
S-3	First and second cycle extraction	High-level liquid waste	200,000 gal	Fission products (15 MT, 1400 MCi); actinides (2 MT, 95 MCi)

Table 14 (continued)

Stream No.	Source (Subsystem)	Waste Form	Approx. Quantities per yr (Est.)	Probable Key Radionuclides Present (Est. Amt/yr)
<u>Solvent Extraction System (cont'd)</u>				
S-4	First and second cycle extraction	Thorium nitrate solution	50,000 gal <sup>b</sup>	Th (155 MT, 60 kCi), Zr, Nb, Ru, Rh, actinides (Total FP, 2 MCi)
S-5	First and second cycle extraction	Kerosene scrub	5,500 gal	Fission products, actinides
S-8	Solvent cleanup	Crud	~ 1 MT	Fission products (2 kg, 150 kCi), actinides (170 kg, 95 kCi)
<u>Off-Gas Cleanup System</u>				
0-1	NO <sub>x</sub> decomposition, catalytic oxidation	Spent catalysts	140 ft <sup>3</sup>	Fission products (esp., semi-volatile)
0-2	Iodine removal	Spent zeolite	Pb zeolite = 1200 ft <sup>3</sup> Ag zeolite = 150 ft <sup>3</sup>	Iodine isotopes (60 Ci, 35 kg)
0-3	Radon removal	Spent molecular sieve	440 ft <sup>3</sup>	Rn daughters, traces of I and HTO
0-4	Tritium removal	Spent molecular sieve	150 ft <sup>3</sup>	HTO
0-5	Tritium removal	Tritiated water	3,700 gal	HTO ( <sup>3</sup> H, 227 kCi)
0-6	Krypton removal	Kr-product stream	Kr: 460 kg	Kr-85 (11 MCi)
0-7	Krypton removal	CO <sub>2</sub> gas	6,680 MT	C-14 (0.3 kg C-14, 1400 Ci), Kr-85 (trace)

Table 14 (concluded)

Stream No.	Source (Subsystem)	Waste Form	Approx. Quantities per yr (Est.)	Probable Key Radionuclides Present (Est. Amt/yr)
<u>Miscellaneous</u>				
M-1	HTGR	Reflector blocks	5600 ft <sup>3</sup> (350 MT)	C-14, neutron-activation products
M-2	Facilities	Decontamination solution	1-2 x 10 <sup>6</sup> gal	Variable
M-3	Facilities	Rags, spent filters, failed equipment and tools, etc.	74,000 ft <sup>3</sup>	Variable

<sup>a</sup> Assume ~5% of the fuel material formed clinkers.

<sup>b</sup> Unconcentrated solutions.

### Fixation of $^{14}\text{C}$ as $\text{CaCO}_3$

A scoping study was conducted to determine the best method for the fixation of  $^{14}\text{C}$ -contaminated  $\text{CO}_2$  as  $\text{CaCO}_3$ , and to evaluate the various options available for disposing of the  $\text{CaCO}_3$  thus produced.<sup>43</sup> The fixation and disposal options were evaluated on the basis of technical merit, economics, and regulatory acceptability.

The two  $\text{CO}_2$  fixation processes considered were:

1. A direct process, wherein the  $\text{CO}_2$  is reacted directly with a slaked lime [ $\text{Ca}(\text{OH})_2$ ] slurry to form a  $\text{CaCO}_3$  slurry.
2. A double alkali process, wherein the  $\text{CO}_2$  is reacted with a  $\text{NaOH}$  solution to form  $\text{Na}_2\text{CO}_3$ ; the  $\text{Na}_2\text{CO}_3$  is subsequently reacted with a slaked lime slurry to produce the  $\text{CaCO}_3$  product and to regenerate the  $\text{NaOH}$  solution.

The direct  $\text{CO}_2$  fixation process appears to be superior to the double alkali process because of reduced complexity, reduced corrosiveness of the chemical reagents involved, and reduced cost. The two processes were judged to be equivalent with respect to the amount of solids handling required. The double alkali process has an advantage with respect to design data availability since the  $\text{NaOH}-\text{CO}_2-\text{H}_2\text{O}$  system has been well characterized.

The  $\text{CaCO}_3$  disposal options considered were as follows:

1. Shallow-land burial of
  - (a) Unpackaged  $\text{CaCO}_3$  (as prepared)
  - (b) Packaged  $\text{CaCO}_3$  (as prepared)
  - (c) Unpackaged  $\text{CaCO}_3$  (fixed in concrete)
  - (d) Packaged  $\text{CaCO}_3$  (fixed in concrete)
2. Hydraulic fracturing (mixing a  $\text{CaCO}_3$  slurry with cement and injecting it into deep geological strata).
3. Deep sea disposal (concretion and dumping in the deep sea).
4. Partial block burning.
5. Emplacement in a geologic repository for material contaminated with alpha emitters.

Shallow land burial of the  $\text{CaCO}_3$  appears to be the best disposal option available. The burial of unpackaged  $\text{CaCO}_3$  [Option 1(a)] will probably

not be acceptable. The future acceptability of burying packaged  $\text{CaCO}_3$  [Option 1(b)] or unpackaged, concreted  $\text{CaCO}_3$  [Option 1(c)] is not clear at the present time. The burial of packaged, concreted  $\text{CaCO}_3$  [Option 1(d)] will probably be acceptable in the future. Thus, the potentially acceptable shallow-land burial options, in decreasing order of economic preference, are:

1. Burial of packaged  $\text{CaCO}_3$  (\$18/kg HM).
2. Burial of unpackaged, concreted  $\text{CaCO}_3$  (\$29/kg HM).
3. Burial of packaged, concreted  $\text{CaCO}_3$  (\$43 to 56/kg HM, depending on whether concretion is done at the burial or processing sites).

The disposal of  $\text{CaCO}_3$  via hydraulic fracturing does not appear to be attractive based on a combination of economic (\$36.78/kg HM), regulatory, and technical grounds. The dumping of the  $\text{CaCO}_3$  in the deep sea does not appear to be attractive on both economic (\$56.43/kg HM) and regulatory acceptance grounds. Partial block burning is unattractive because the maximum volume reduction is only about 50% and the fission products sorbed on the unprocessed blocks elevate the waste from the low-level category to at least the intermediate level. The geologic-repository burial of the  $\text{CaCO}_3$  is economically unattractive (\$280/kg HM) and technically unjustifiable in view of the relatively low toxicity of  $^{14}\text{C}$ .

The feasibility of placing the  $\text{CO}_2$  fixation system before the Kr removal system to reduce or eliminate the gas volume which the Kr removal system must handle was also investigated. The process complexity and increased cost resulting from this change indicate that it would be more advantageous to put the  $\text{CO}_2$  fixation process after the Kr removal process.

#### Controlled Release of $^{14}\text{CO}_2$

A detailed analysis<sup>44</sup> of the local radiological impact of released  $^{14}\text{CO}_2$  indicates that the timing of the release will strongly influence the maximum dose. Because of the limitation of photosynthesis to daylight hours, daytime release during the growing season will result in increased

uptake of  $^{14}\text{C}$  by local vegetation, and hence an increased transfer into the food-chain pathway, which ordinarily accounts for more than 99% of the  $^{14}\text{C}$  dose to man. Therefore, this analysis suggests that significant local-dose benefits are obtainable from daytime holdup and nocturnal release of  $^{14}\text{CO}_2$ .

#### ACKNOWLEDGEMENTS

The work described here was performed by about 20 staff members of the Chemical Technology Division, whose names are included among the references. Three guest scientists also participated in this work: H. Barnert-Wiemer (KFA-Jülich), D. M. Levins (Australian AEC), and H. W. R. Beaujean (KFA-Jülich).

## REFERENCES

1. K. J. Notz, An Overview of HTGR Fuel Recycle, ORNL-TM-4747 (January 1976).
2. V. C. A. Vaughen, J. R. Flanary, J. H. Goode, and H. O. G. Witte, Hot Cell Evaluation of the Burn-Leach Method for Reprocessing Irradiated Graphite-Base HTGR Fuels, ORNL-4120 (February 1970).
3. C. L. Fitzgerald and V. C. A. Vaughen, Head-End Reprocessing Studies with Irradiated HTGR Fuels: II. Studies with Dragon Fuel Compacts, ORNL-5004 (to be issued).
4. C. L. Fitzgerald, V. C. A. Vaughen, K. J. Notz, R. S. Lowrie, Head-End Reprocessing Studies with Irradiated HTGR-Type Fuels: III. Studies with RTE-7: TRISO UC<sub>2</sub>-TRISO ThC<sub>2</sub>, ORNL-5090 (November 1975).
5. C. L. Fitzgerald and R. D. Arthur, (internal program report) Head-End Reprocessing Studies with H-1 and H-2 Capsules, BISO-Coated UO<sub>2</sub>, ThO<sub>2</sub> and (2.2-4.1 Th,U)O<sub>2</sub> Fuel Combinations, GCR: 75-40 (February 1976).
6. C. L. Fitzgerald and V. C. A. Vaughen, (internal program report) Information and Data for Primary and Secondary Burner Off-Gas Streams - Preliminary Data for Program Request ACC-ORNL-3, GCR: 74-39 (December 1974).
7. C. L. Fitzgerald and V. C. A. Vaughen, (internal program report) Information and Data for HTGR Fuel Burner Off-Gas Streams: Final Response to Program Request ACC-ORNL-3, GCR: 75-16 (May 1975).
8. E. E. McCombs, (internal program report) Fission Product and Actinide Volatility During HTGR Burner Operation: An Experimental Procedure, GCR: 75-32 (October 1975).
9. M. Laser, H. Barnert-Wiemer, H. Beaujean, E. Merz, H. Vygen, "AKUT: A Process for the Separation of Aerosols, Krypton and Tritium from Burner Off-Gas in HTR Fuel Reprocessing," Proceedings of the Thirteenth AEC Air Cleaning Conference, San Francisco, 12-15 Aug. 1974, CONF-740807, Vol. 1, pp. 236-262 (March 1975).
10. R. W. Glass et al., HTGR Head-End Processing: A Preliminary Evaluation of Processes for Decontaminating Burner Off-Gas, ORNL-TM-3527 (July 1972).
11. K. J. Notz, A. B. Meservey, and R. D. Ackley, "The Solubility of Krypton and Xenon in Liquid CO<sub>2</sub>," ANS 1973 Winter Meeting; published in Trans. Am. Nucl. Soc. 17, 318-19 (November 1973).

12. D. E. Ferguson, P. A. Haas, and R. E. Leuze, "Quantitative Recovery of Krypton from Gas Mixtures Mainly Comprising Carbon Dioxide," U.S. Patent 3,742,720 (July 3, 1973).
13. M. E. Whatley, Calculations on the Performance of the KALC Process, ORNL-4859 (April 1973).
14. R. W. Glass, T. M. Gilliam, and V. L. Fowler, An Empirical Model for Calculating Vapor-Liquid Equilibrium and Associated Phase Enthalpy for the CO<sub>2</sub>-O<sub>2</sub>-Kr-Xe System for Application to the KALC Process, ORNL-TM-4947 (January 1976).
15. J. C. Mullins and R. W. Glass, An Equilibrium Stage Model of the KALC Process, ORNL-TM-5099 (in preparation).
16. K. J. Notz and A. B. Meservey, The Solubility of Krypton in Liquid CO<sub>2</sub>, ORNL-5121 (in reproduction).
17. R. D. Ackley and K. J. Notz, The Distribution of Xenon Between Gaseous and Liquid CO<sub>2</sub>, ORNL-5122 (in preparation).
18. R. W. Glass et al., System Features and Component Descriptions for the Unit Operations Off-Gas Decontamination Facility, ORNL-TM-4596 (February 1975).
19. D. M. Levins, R. W. Glass, M. M. Chiles, and D. J. Inman, Monitoring and Analysis of Process Streams in a Krypton-85 Off-Gas Decontamination System, ORNL-TM-4923 (July 1975).
20. R. W. Glass et al., Krypton Absorption in Liquid CO<sub>2</sub> (KALC): Campaign II in the Experimental Engineering Section Off-Gas Decontamination Facility, ORNL/TM-5095 (February 1976).
21. H. D. Cochran, Jr., and A. D. Ryon, (internal program report) Final Report on the KALC Campaign at the ORGDP Off-Gas Pilot Plant May to June 1974, GCR: 74-41 (January 1975).
22. A. D. Ryon, KALC Campaign II at the ORGDP Off-Gas Pilot Plant, ORNL/TM-5298 (in preparation).
23. C. W. Forsberg, (internal program report) Selection of a Process to Remove Carbon Dioxide from a Krypton Gas Mixture, GCR: 76-4 (in preparation).
24. W. S. Groenier and B. A. Hannaford, An Engineering Evaluation of the Iodex Process: Part II: Removal of Iodine from Air Using a Nitric Acid Scrub in a Bubble Cap Column; Part III; Correlation of Mass Transfer Data; Part IV: Process Sensitivity to Impurities, ORNL-TM-4701 (May 1975).

25. B. A. Hannaford and W. S. Groenier, (internal program report) in Monthly Progress Report for the Gas-Cooled Reactor Programs at Oak Ridge National Laboratory, GCR: 74-13 (April 1974), p. 4.
26. J. T. Bell and L. M. Toth, in Chemical Technology Division Annual Progress Report for Period Ending March 31, 1974, ORNL-4966, pp. 49-51.
27. J. T. Bell and L. M. Toth, in Chemistry Division Annual Report for Period Ending November 1, 1975, ORNL-5111 (February 1976).
28. H. Barnert-Wiemer, Experimental Studies of a One-Sixth-Scale Whole-Block Burner, Appendix to ORNL-TM-4520 (November 1974).
29. J. W. Snider and D. C. Watkin, An Evaluation of HTGR Primary Burning, ORNL-TM-4520 (November 1974).
30. Paul A. Haas, HTGR Fuel Reprocessing: A Whole-Block Burner with Recycle of Cooled Gas for Temperature Control, ORNL-TM-4519 (August 1974).
31. R. M. Canon, in Experimental Engineering Section Semiannual Progress Report (Excluding Reactor Programs) for Period September 1, 1974 to February 28, 1975, ORNL-TM-4961 (December 1975), pp. 381-7.
32. R. M. Canon, in Experimental Engineering Section Semiannual Progress Report (Excluding Reactor Programs) for Period March 1, 1975 to August 31, 1975, ORNL-TM-5291 (in preparation).
33. J. M. Kuchta, A. Kant, and G. H. Damon, "Combustion of Carbon and High Temperature, High Velocity Air Streams," Ind. Eng. Chem. 44(7), 1559 (1952).
34. W. S. Groenier, Calculation of the Transient Behavior of a Dilute-Purex Solvent Extraction Process Having Application to the Reprocessing of LMFBR Fuels, ORNL-4746 (April 1972).
35. G. L. Richardson and J. L. Swanson, Plutonium Partitioning in the Purex Process with Hydrazine Stabilized Hydroxylamine Nitrate, HEDL-TME-75-31, Hanford Engineering Development Lab. (1975).
36. S. B. Watson and R. H. Rainey, Modifications of the SEPHIS Computer Code for Calculating the Purex Solvent Extraction System, ORNL-TM-5123 (December 1975).
37. T. V. Healy and H. A. C. McKay, "Complexes Between Tributyl Phosphate and Inorganic Nitrates," Rec. Trav. Chim. 75, 730 (1956).
38. R. H. Rainey, "Combining Ratio of TBP and DSBPP and Thorium Nitrate," in Chemical Technology Division, Quarterly Progress Report for Chemical Development Section B, October-December 1962, ORNL-TM-545, pp. 26-31 (September 1963).

39. W. L. Carter, (internal program report) Comparison of Inert Gas Sparge and Ion Exchange to Reduce  $^{232}\text{U}$  Daughter Activity in  $^{233}\text{UO}_2(\text{NO}_3)_2$  Solutions, GCR: 75-12 (April 1975).
40. W. L. Carter, (internal program report) HTGR Fuel Reprocessing and Refabrication: Technical Elements Pertinent to  $^{220}\text{Rn}$  Control in Off-Gas Streams, GCR: 75-15 (August 1975).
41. K. H. Lin, (internal program report) Identification and Characterization of Waste Streams from an HTGR Fuel Reprocessing Plant, GCR: 75-23 (August 1975).
42. K. H. Lin, Characteristics of Radioactive Waste Streams Generated in HTGR Fuel Reprocessing, ORNL-TM-5096 (January 1976).
43. A. G. Croff, An Evaluation of Options Relative to the Fixation and Disposal of  $^{14}\text{C}$ -Contaminated  $\text{CO}_2$  as  $\text{CaCO}_3$ , ORNL/TM-5171 (in preparation).
44. G. G. Killough, K. R. Dixon, N. T. Edwards, B. D. Murphy, P. S. Rohwer, W. F. Harris, and S. V. Kaye, Progress Report on Evaluation of Potential Impact of  $^{14}\text{C}$  Releases from an HTGR Reprocessing Facility, ORNL-TM-5284 (in preparation).



## INTERNAL DISTRIBUTION

- |                        |                                 |
|------------------------|---------------------------------|
| 1. R. D. Ackley        | 27-29. P. R. Kasten             |
| 2. J. O. Blomeke       | 30-33. R. K. Kibbe, GAC/ORNL    |
| 3-7. R. A. Bradley     | 34. W. J. Lackey                |
| 8. R. E. Brooksbank    | 35. K. H. Lin                   |
| 9. W. D. Burch         | 36. A. L. Lotts                 |
| 10. R. M. Canon        | 37. A. P. Malinauskas           |
| 11. W. L. Carter       | 38. E. E. McCombs               |
| 12. J. H. Coobs        | 39-71. K. J. Notz               |
| 13. A. G. Croff        | 72. A. R. Olsen                 |
| 14. F. L. Culler       | 73. W. H. Pechin                |
| 15. W. Davis, Jr.      | 74. H. Postma                   |
| 16. F. E. Dearing, Jr. | 75. R. H. Rainey                |
| 17. D. E. Ferguson     | 76. A. D. Ryon                  |
| 18. C. L. Fitzgerald   | 77. C. D. Scott                 |
| 19. C. W. Forsberg     | 78. J. D. Sease                 |
| 20. T. M. Gilliam      | 79. J. H. Shaffer               |
| 21. R. W. Glass        | 80. D. B. Trauger               |
| 22. W. S. Groenier     | 81. V. C. A. Vaughen            |
| 23. P. A. Haas         | 82. R. G. Wymer                 |
| 24. F. E. Harrington   | 83-84. Central Research Library |
| 25. C. C. Haws         | 85. Document Reference Section  |
| 26. F. J. Homan        | 86-87. Laboratory Records       |
|                        | 88. Laboratory Records (RC)     |
|                        | 89. ORNL Patent Section         |

## CONSULTANTS

- 90. W. K. Davis
- 91. J. C. Frye
- 92. C. H. Ice
- 93. J. J. Katz
- 94. R. B. Richards

## EXTERNAL DISTRIBUTION

- 95. Research and Technical Support Division, ERDA, ORO
- 96. Director, Reactor Division, ERDA, ORO
- 97-98. Director, Reactor Research and Development, ERDA  
Washington, D.C. 20545
- 99-100. Director, Division of Nuclear Fuel Cycle and Production, ERDA,  
Washington, D.C. 20545
- 101-267. Given distribution as shown in TID-4500 under Gas-Cooled Reactor  
Technology category
- 268-305. U.S./German HTR Research Exchange Agreement (TIC to distribute)